Pathological study on the toxicity of 1-methyl-4-phenyl-1,2,3,6-tetrahydropyridine (MPTP) and 6-hydroxydopamine (6-OHDA) upon the nigrostriatal dopaminergic system of the golden hamster

(ゴールデンハムスターの黒質線条体系における
1-methyl-4-phenyl-1,2,3,6-tetrahydropyridine (MPTP) と 6-hydroxydopamine (6-OHDA)
の毒性発現に関する病理学的研究)

Rodríguez Sebastián
ロドリゲス　セバスティアン

Contents

General Introduction

Parkinson's disease (PD) is the second most common neurodegenerative disorder in humans over 65 years old. Traditionally, PD is classified into two different types: familial and sporadic. On the one hand, familial PD is a term used to characterize PD in the setting of a known family history of one or more affected relatives [1]. On the other hand, sporadic PD, the most common presentation of this neurodegenerative disorder, has been suggested as a consequence resulting from complex interactions between gene susceptibility and environmental factors. Interestingly, recent studies have also suggested that patients with sporadic PD often display a coexisting metabolic dysfunction, which may exacerbate neurological symptoms [2].

The main pathomorphological alteration in patients with PD is the depletion of dopaminergic neurons located in the substantia nigra pars compacta (SNpc) with the consequent deficit of dopamine in the caudate putamen (striatum) [3]. A nigrostriatal deficit of the dopamine metabolites homovalinic acid (HVA) and 3,4-dihydroxyphenylacetate (DOPAC), as well as a depletion in dopamine transporters, have also been described [1]. In addition, it is now apparent that another pathological hallmark of PD, observed in the brain of PD patients as well as of PD animal models, is

the infiltration of inflammatory cells and astrocytes [4-5].

In spite of the important progresses in the pathogenesis of PD, the aetiology(ies) of this disorder remains to be elucidated. Indeed, the use of animal models, especially those in which neurotoxins are employed to reproduce the pathological hallmarks of PD and to induce parkinsonian syndrome (bradykinesia, rest tremor, rigidity and postural instability [6-7]), offers insights into the complex pathology and molecular mechanisms of PD. In this regard, two of the most important neurotoxin-based models are the 1-methyl-4-phenyl-1,2,3,6-tetrahydropyridine (MPTP) and the 6-hydroxydopamine (6-OHDA) models where lesions of the nigrostriatal axis are observed when these neurotoxins are systemically and intrastriatally injected, respectively.

Modeling PD using MPTP

MPTP was successfully used to model PD in squirrel monkeys in 1984 [8]. Since then it has been very widely used for replicating almost all the hallmarks of PD. MPTP, which itself is non-toxic, passes through the blood brain barrier (BBB) and is metabolized into 1-methyl-4-phenylpyridinum (MPP^+) (the active neurotoxin) by the astrocytic monoamine oxidase-B (MAO-B) [9-10]. Once converted, MPP^+ is taken up

into dopaminergic neurons where inhibits complex I of the mitochondrial electron transport chain [11]. However, neurotoxicity of MPTP also depends on the contents of cerebral capillary MAO-B: if the levels of the enzyme are increased in the BBB endothelial cells, MPTP may be converted to MPP^+ at this site and, due to its polarity and ionic charge, MPP^+ cannot cross through the BBB [12-13].

Interestingly, while C57BL/6 mice show a high sensitivity to MPTP, most of the rodent species are exceptionally resistant to the systemic administration of this toxin. A faster clearance of MPTP metabolites in the caudate area [14] and the ability of catecholamine neurons to cope with impaired energy metabolism [15] have been proposed as potential mechanisms involved in the resistance of some rodents to MPTP-induced neurotoxicity. As far as the golden hamster (GH) is concerned, Mitra *et al*. [16] demonstrated that, after an acute or chronic subcutaneous treatment with MPTP, the nigrostriatal axis of this species remains unaffected.

Modeling PD using 6-OHDA

Neurotoxic effects of 6-OHDA upon nigrostriatal dopaminergic cells in the rat and mouse have been fully described [17-24]. The underlying assumption is that 6-OHDA

exerts its effects via the generation of hydrogen peroxide and other derived oxyradicals [25-30], which selectively destroy nerve cell endings of sympathetic neurons [31] and induce a permanent degeneration of the nigrostriatal pathway [32-33]. Because of its incapability to pass through the BBB [34], 6-OHDA is administered directly into the striatum, SNpc or medial forebrain bundle (MFB) to induce parkinsonism. However, despite the widespread use in the rat, only few studies about 6-OHDA-induced neurotoxicity have been carried out in other rodent species and, to this end, there have been no reports describing its potential effects on the nigrostriatal axis of the GH.

Overview of the thesis contents

This thesis, which consists of four chapters, is designed in order to study the effects of MPTP and 6-OHDA in the GH that, so far, has been an under-utilized model for studies in neuropathology.

Despite a previous report [16] stated that the GH is resistant to MPTP-induced neurotoxicity due to the low levels of cerebral MAO-B, to date, there have been no other studies to deepen the understanding of this resistance. For this reason, **Chapter 1** is undertaken to extend the knowledge of the GH resistance to MPTP.

Chapter 2 is designed with the aim of evaluating, for the first time, the effects of a single intrastriatal injection of 6-OHDA in the young-adult GH and to present a time-course analysis of the tyrosine hydroxylase (TH) and dopamine transporter (DAT) loss in the nigrostriatal axis.

Since the loss of dopamine cells in the human sporadic PD has been associated with programmed cell death (PCD) and active immune response in the nigrostriatal axis, **Chapter 3** is designed with the aim of evaluating the histopathological characteristics of cell death and inflammation using the novel GH hemiparkinsonian 6-OHDA model presented in Chapter 2.

Finally, the major purpose of **Chapter 4** is to analyze whether the attenuation of neuroinflammation influences the onset and progression of the dopamine cell degeneration induced by 6-OHDA intrastriatal injection.

This thesis provides advances in the understanding of the GH resistance to MPTP and in the potential mechanisms involved in the development of 6-OHDA-induced dopaminergic cell degeneration.

Abbreviations used in this thesis

6-OHDA: 6-hydroxydopamine

BBB: blood brain barrier

BDNF: brain-derived neurotrophic factor

DAT: dopamine transporter

GDNF: glial-derived neurotrophic factor

GFAP: glial fibrillary acidic protein

GH: golden hamster

H&E: hematoxylin-eosin stain

iNOS: inducible oxide nitric synthase

MAO-A: monoamine oxidase A

MAO-B: monoamine oxidase B

MINO: minocycline

MINO+Pred: minocycline + prednisolone treatment

MPTP: 1-methyl-4-phenyl-1,2,3,6-tetrahydropyridine

MPP^+: 1-methyl-4-phenylpyridinum

PD: Parkinson's disease

Pred: prednisolone

RNS: reactive nitrogen species

ROS: reactive oxygen species

SNpc: substantia nigra pars compacta

SVZ: subventricular zone

TH: tyrosine hydroxylase

TNF-α: tumor necrosis factor alpha

Chapter 1

Resistance of the GH to MPTP-induced neurotoxicity is not only related with low levels of cerebral MAO-B

Abstract

Studies about the neurotoxicity of MPTP in GH demonstrated that the nigrostriatal axis was unaffected after acute and chronic subcutaneous treatments with this toxin. The low levels of cerebral MAO-B (insufficient to oxidize MPTP to MPP^+) were proposed as the cause of this resistance. To elucidate whether MAO-B is the only factor which confer GH resistance to MPTP, female and male GH were intracerebroventricularly (icv) injected with either MPTP or MPP^+. The results show that neither depletion in the number of dopaminergic neurons in the nigrostriatal axis nor cell death in the SVZ occurred after an icv treatment with MPTP or MPP^+. In addition, double-labeling immunofluorescent histochemistry was performed in order to elucidate the localization of MAO-B in the brain. This staining revealed that MAO-B is not expressed within the astroglia, but in the endothelial cells and pericytes in the BBB. Taken together, these results raise the possibility that other mechanisms, apart from the low levels of regional MAO-B, confer GH resistance to MPTP and its toxic metabolite.

Introduction

While some strains of mice (such as C57BL/6) show a high sensitivity to MPTP [35], most of the rodent species exhibit low susceptibility to this toxin. A faster clearance of MPTP metabolites from the caudate area [14] and the ability of catecholamine neurons to cope with impaired energy metabolism [15] have been proposed as potential mechanisms to explain the rodent's resistance to MPTP and MPP^+. One hypothesis to explain the resistance to MPTP observed for the GH is that MAO-B is slightly expressed in astrocytes and that a high MAO-A to MAO-B ratio (relative dominance of MAO-A) predominates in the brain of this species [16].

In the present chapter, I investigated whether MAO-B is the only critical factor in determining the resistance of the GH to MPTP.

Materials and methods

Animals

Eight-week-old female and male golden hamsters (Mesocricetus auratus), weighing 90-130 g (SLC, Tokyo, Japan) were housed in a temperature-controlled room (23 ± 2 °C) with a constant level of humidity (55 ± 5%) under a 12/12 h light/dark cycle and ad libitum access to food and water. All the procedures used in this study were approved by the Committee of Animal Experiments, Graduate School of Agricultural and Life Science, The University of Tokyo.

Experimental design

The diagram of the experimental design used in this work is summarized in **table 1.1**. Briefly, to carry out an acute intraperitoneal (ip) MPTP treatment on female GH, 20 mg/kg of MPTP-HCl (Sigma, St. Louis, MO) were dissolved in 10 ml/kg body weight of saline solution and administered two or four times at two-hour intervals within a single day, for a cumulative dose of 40 mg/kg or 80 mg/kg, respectively. Control GH received saline injections only. To perform the intracerebroventricular (icv) injections, female and male GH were deeply anesthetized with 4% chloral hydrate (360 mg/kg,

MYLAN, Osaka, Japan) and injected once with either MPTP-HCl or MPP^+ (Sigma, St. Louis, MO) using the following coordinates with respect to the bregma: 0.5 mm anterior; 1.8 mm lateral; 4.0 mm deep from the surface of the skull. After a continuous MPTP or MPP^+ injection flow (2µl/min) using a Hamilton microliter syringe (Hamilton Company, Reno, Nevada 89502, USA), the needle was kept for 5 minutes in the site of injection and then carefully removed from the cavity. Control group received saline icv injection only. The final volume of injected solution in each animal was 20 µl.

Tissue preparation

All the animals were euthanized by a cervical dislocation after being deeply sedated with diethyl ether. The brains were immediately isolated, fixed in 10% neutral buffered formalin, embedded in paraffin and cut into coronal sections encompassing the entire SVZ and SNpc. The sections were used for TUNEL, immunohistochemistry and immunofluorescence tests.

Immunohistochemistry

Paraffin sections were used for immunohistochemistry with the following primary antibodies: i) rabbit anti-TH (1:400; Millipore, Temecula, CA) as a marker for

dopaminergic neurons and, ii) rabbit anti-GFAP (1:200; DAKO, Carpinteria, CA) as a marker for astrocytes. After deparaffinized, the sections were subjected to a heat-induced epitope unmasking in 10 nM citrate buffer (pH 6.0) in autoclave at 121 °C for 10 min, then treated with 10% hydrogen peroxide/methanol for 5 min to inactivate endogeneous peroxidase, and incubated in 8 % skim milk/TBS at 37 °C for 40 min to block non-specific binding of the antibodies. The tissue sections were incubated at 4 °C overnight with the first antibodies diluted in TBS, and then developed using the anti-rabbit HRP Envision System (DAKO, Carpinteria, CA) for 40 min. Finally, the sections were visualized by 0.05% 3,3´-diaminobenzidine (DAB) with 0.03% hydrogen peroxide in Tris–HCl buffer, and followed by conterstaining with 5 % methyl green (pH 4.0).

Double-labeling immunofluorescence

To determine the distribution of MAO-B, double-labeling immunofluorescent histochemistry was carried out using the following primary antibodies: i) goat anti-MAO-B (1:10, Santa Cruz Biotechnology, Santa Cruz, CA); ii) rabbit anti-GFAP (1:200, DAKO), as a marker for astrocytes and, iii) rabbit anti-CD-31 (Ready-to-use,

Invitrogen, Carlsbad, CA), as a marker for endothelial cells. Four µm thick-paraffin sections were autoclaved at 121°C for 15 min for antigen retrieval and subsequently treated with skimmed milk at 37°C for 40 min in order to block non-specific reactions. Subsequent to overnight incubation with the first antibodies, samples were incubated at room temperature for 1h with the following secondary antibodies: i) donkey anti-rabbit Alexa 594 red (1:00, Invitrogen, Carlsbad, CA) and, ii) donkey anti-goat Alexa 488 green (1:100, Invitrogen, Carlsbad, CA). Sections were then mounted with Vectashield (Vector Laboratories, Burlingame, CA) and observed using the Zeiss LSM510 confocal laser scanning microscope.

TUNEL method

Apoptotic cells containing fragmented DNA were detected using the TUNEL method with the ApopTag Peroxidase In Situ Apoptosis Detection Kit (Chemicon, Temecula, CA) according to the manufacturer's instructions. Negative controls were processed in parallel with the use of saline solution instead of Tdt enzyme. Tissue sections were finally counterstained with 5% methyl green solution pH 4.0.

Measurements and statistics

Serial brain coronal tissue sections (including the SVZ and the SNpc) were collected with the aid of “A stereotaxic atlas of the golden hamster brain” [36]. At least 4 sections per animal were blindly applied for a quantitative analysis of TH-positive cells, TH positive area, GFAP positive area or TUNEL-positive cells. In the SNpc, the cells were measured using a manual counter (TTS, Osaka, Japan) and the results were expressed as the mean number of TH-positive cells ± standard deviation (SD). In the SVZ, TH-positive area or GFAP-positive area were measured using the ImageJ software version 1.44t (http://rsb.info.nih.gov/ij/). The results were expressed as the mean ± SD. Two-way ANOVA test was used to assess the differences between data groups. Potential differences between control and MPP^+ group in the TUNEL assay were calculated using Student’s t-test. Differences were considered statistically significant when $p < 0.05$.

Results

Clinical symptoms

MPTP (ip and icv) or MPP^+ (icv) administration caused neither tremor nor impaired locomotor activity in female or male GH. No other clinical signs related with neurotoxicity were recorded.

Effects of acute MPTP ip treatment upon female GH

There was no loss of TH-positive cells in the SNpc of two-MPTP injections (x2) or four-MPTP injections (x4) groups **(Fig. 1-1)**. In concordance with the findings in the SNpc, there was no decrease of the TH-positive areas in the MPTP-treated groups **(Fig. 1-2)**. Furthermore, no increases of the GFAP-positive areas were detected (**Fig. 1-3**).

Very few TUNEL-positive cells in the SVZ were detected in treated animals (MPTP x2 and MPTP x4) and no statistical differences were recorded **(Fig. 1-4).**

Effects of acute MPTP or MPP^+ icv treatment upon female and male GH

There were no significant differences in the number of TH-positive cells in the SNpc **(Fig. 1-5)** or in the TH-positive areas in the striatum **(Fig. 1-6**) when GHs were injected with either MPTP or MPP^+.

In addition, there were no significant differences in the number of TUNEL-positive cells in the SVZ of MPP^+-treated female or male GHs (**Fig. 1-7**).

MAO-B localization

Double-labeling immunofluorescent histochemistry revealed that MAO-B is not expressed within the astroglia **(Fig. 1-8)**, but in the endothelial cells and pericytes (**Fig. 1-9).**

Discussion

In the present chapter I demonstrated that, in the GH's brain, the enzyme MAO-B, responsible for the conversion of MPTP to MPP^+, is expressed in the endothelial cells. This observation suggests that endothelial cells in the BBB convert MPTP to MPP^+ and may explain part of the GH resistance to systemically administered MPTP. In addition, I demonstrated that GH is also resistant to icv-injected MPP^+, which suggests that other mechanism/s contribute to the resistance of GH to MPTP and its toxic metabolite.

In the only published report of the effects of MPTP in GH, Mitra *et al*. [16] proposed that the low levels of MAO-B confer GH resistance to this neurotoxin. Differences in the MPTP neurotoxicity between species due to the levels of MAO-B activity have been described in previous reports [37-38]. It is well established that only MAO-B converts MPTP to MPP^+ within the glial cells [10, 39-40], and this step is a *sine qua non* condition for MPTP to exert its neurotoxicity. MAO-B inhibitors, such as pargyline and selegiline, have been used to confer resistance against MPTP [41-42]. Moreover, the importance of MAO-B inhibition to alleviate symptoms in patients with idiopathic PD has been previously postulated [43-44].

The endothelial cells in the BBB have been suggested to be the first potential site for detoxification of neurotoxins [45]. In rats, both isoforms of MAO (A and B) have been found in the microvessels of the BBB, with a preponderance of MAO-B in the postnatal development [46]. If the endothelial cells contain high levels of MAO-B, MPTP injected systemically is converted to MPP^+ at this site, being incapable of crossing the BBB [47]. To exert neurotoxic effects *in vivo*, MPTP passes across the BBB and enters into the glial cells through monoamine or glutamate transporters [10, 48] or pH-dependent antiporters [49-50]. Once into the glial cells, MPTP could be easily converted to MPP^+ by MAO-B. In this research, using double-labeling immunofluorescence, MAO-B was shown to be located predominantly within the endothelial cells and pericytes in the BBB microvasculature, but not into the GFAP-positive cells. This result might explain, at least in part, why systemically injected MPTP in GH does not induce any change in the nigrostriatal axis.

In order to prove whether MAO-B is the only factor implicated in the GH resistance to MPTP, MPP^+ icv administration was performed. Sonsalla *et al*. [51] have shown that icv delivery of MPP^+ in rats induces a dose-dependent ipsilateral loss of

dopaminergic neurons with the concomitant loss of TH-immunoreactivity in the SNpc. In the present study, neither MPTP nor MPP^+ induced changes in the nigrostriatal pathway. Moreover, although nigral degeneration in the idiopathic PD and PD animal models has been associated with gliosis and microvascular proliferation [52-53], no changes occurred in the GFAP-positive areas in the striatum of GH treated with MPTP or MPP^+. These results suggest the possibility that other mechanisms, aside from the low levels of cerebral MAO-B, confer GH resistance to MPTP. In mice, dopamine transporter (DAT), which is highly expressed on dopaminergic neurons, has been proposed as a mandatory component for the MPTP toxicity *in vivo*. The low expression of this transporter could confer resistance against MPTP [54]. Another proposed cytoprotective mechanism is the accumulation of MPP^+ within intracellular vesicles through the vesicular monoamine transporter (VMAT2) [55]. This transporter has been proved to play an important role in the MPTP-induced neurotoxicity *in vivo* because heterozygotes of the VMAT2 knockout mice (VMAT2+/-) showed more sensitivity to the toxin than their wild-type littermates (+/+) [56-57]. In addition, recent studies in the MPTP mouse model of PD have demonstrated that dopaminergic cells may combat the

oxidative stress induced by MPTP through the increased transcription of antioxidant elements (such as Nrf2), and the astrocytic Nrf2 has been implicated in the protection against neurodegeneration [58]. Further studies on dopaminergic neuron receptors, VMAT2 transporters and antioxidant response elements in GH may enhance the understandings of the complete protective mechanisms against MPTP-neurotoxicity in this species.

The number of apoptotic neuroblasts in the SVZ of GH after a treatment with MPTP (ip and icv) or MPP^+ (icv) showed no differences when compared with controls. Although there are conflicting evidences about what kind of mechanisms are implicated in the neuroblastic apoptosis induced by MPTP, studies performed in this laboratory [59-60] have shown that, in C57BL/6 mice, one single injection of MPTP induces apoptosis in both SVZ and rostral migratory stream (RMS). No relationship between DAT expression and MPTP-induced apoptosis in the SVZ of the C57BL/6 mice have been also reported [61]. The results of the present study suggest that, in GH, nigrostriatal dopaminergic neurons and migrating neuroblasts in the SVZ are resistant to MPTP, even though they might differ in their resistance-mechanisms.

In conclusion, the results of the present chapter suggest that other factors, apart from the low levels of cerebral MAO-B, may play a major role in the resistance of the GH to MPTP-induced neurotoxicity.

Table 1.1. Summary of the experimental design

Experimental groups*	Inoculation route**	Inoculated dose	Number (n)	Sacrifice days post injection	Tests
Female MPTP	ip	20 mg/kg (two times)***	3	5	TH+ cells in the SNpc, TH+ and GFAP+ areas in the SVZ
Female MPTP	ip	20 mg/kg (four times)***	3	5	TH+ cells in the SNpc, TH+ and GFAP+ areas in the SVZ
Female MPTP	ip	20 mg/kg (two times)***	3	5	TUNEL+ cells in the SVZ
Female MPTP	ip	20 mg/kg (four times)***	3	5	TUNEL+ cells in the SVZ
Female MPTP	icv	6.9 mg/kg	3	5	TH+ cells in the SNpc, TH+ and GFAP+ areas in the SVZ
Female MPP_+	icv	0.8 mg/kg	7	5	TH+ cells in the SNpc, TH+ and GFAP+ areas in the SVZ
Female MPP_+	icv	0.8 mg/kg	3	1	TUNEL+ cells in the SVZ
Male MPTP	icv	6.9 mg/kg	3	5	TH+ cells in the SNpc, TH+ and GFAP+ areas in the SVZ
Male MPP_+	icv	0.8 mg/kg	7	5	TH+ cells in the SNpc, TH+ and GFAP+ areas in the SVZ
Male MPP_+	icv	0.8 mg/kg	3	5	TUNEL+ cells in the SVZ

* Control groups received the same dose as their counterpart.

** ip = itraperitoneal administration. icv = intracerebreoventricular administration.

*** The interval between injections was two hours.

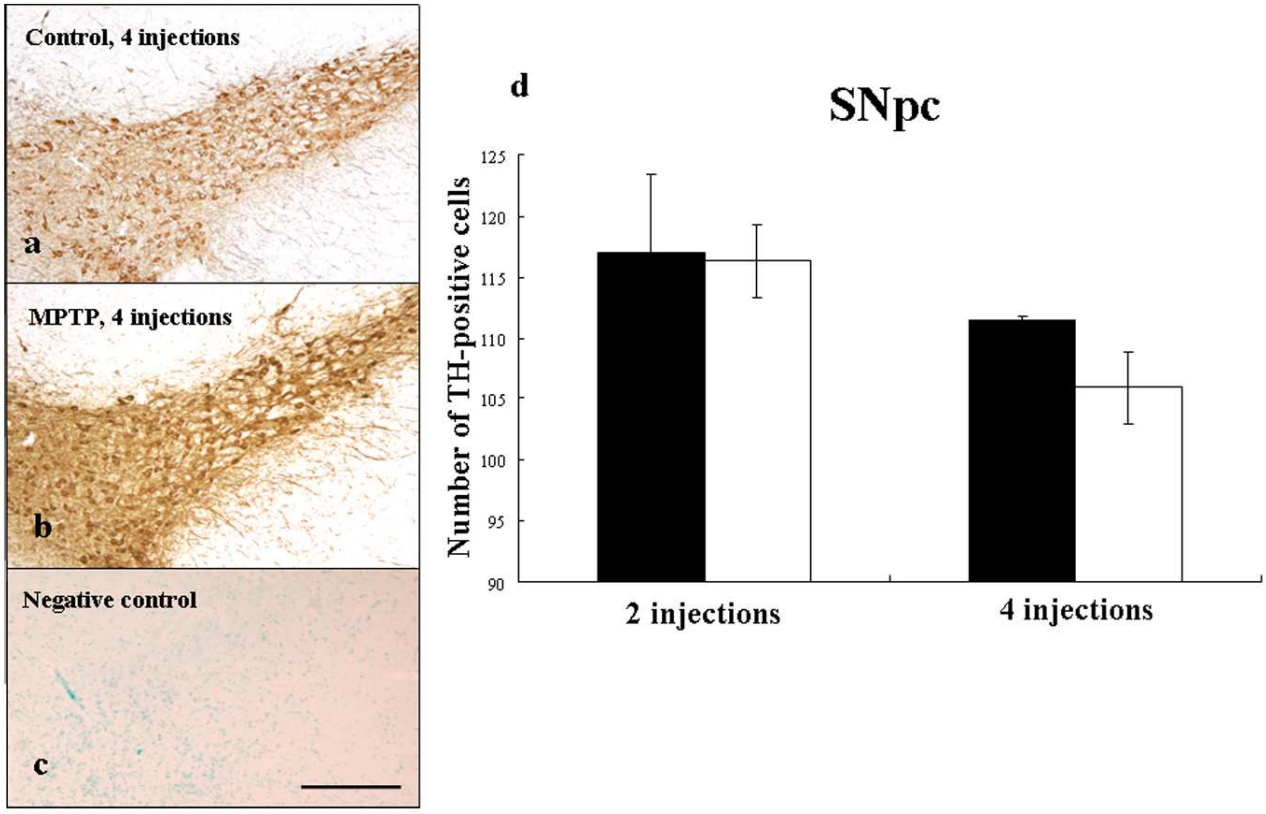

Figure 1-1. Results of TH-immunostaining in the SNpc after an acute ip treatment with MPTP (**a** and **b**) and photomicrograph of a negative control (**c**) to show the lack of TH-unspecific binding. Bar = 300 µm. Figure **d** shows the quantitative analysis of TH-positive cells in the SNpc. The number of TH-positive cells is represented as the mean±SD (n = 3). No significant differences are observed between MPTP-treated GH and controls. ■ = control; □ = MPTP.

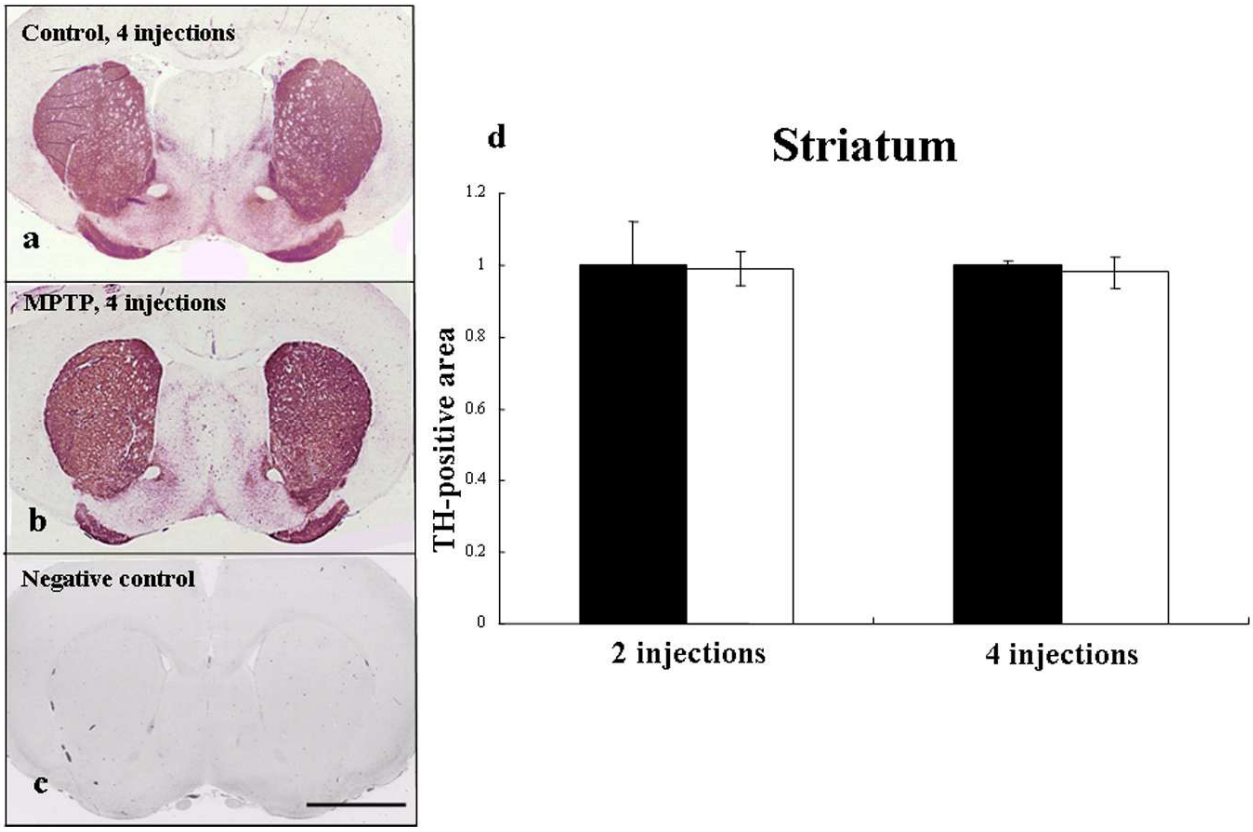

Figure 1-2. Results of TH-immunostaining in the striatum after an acute ip treatment with MPTP (**a** and **b**) and photomicrograph of a negative control (**c**) to show the lack of TH-unspecific binding. Bar = 20 mm. Figure **d** shows the quantitative analysis of TH-positive areas, which are represented as the mean±SD (n = 3). No significant differences are observed between MPTP-treated GH and controls. ■ = control; □ = MPTP.

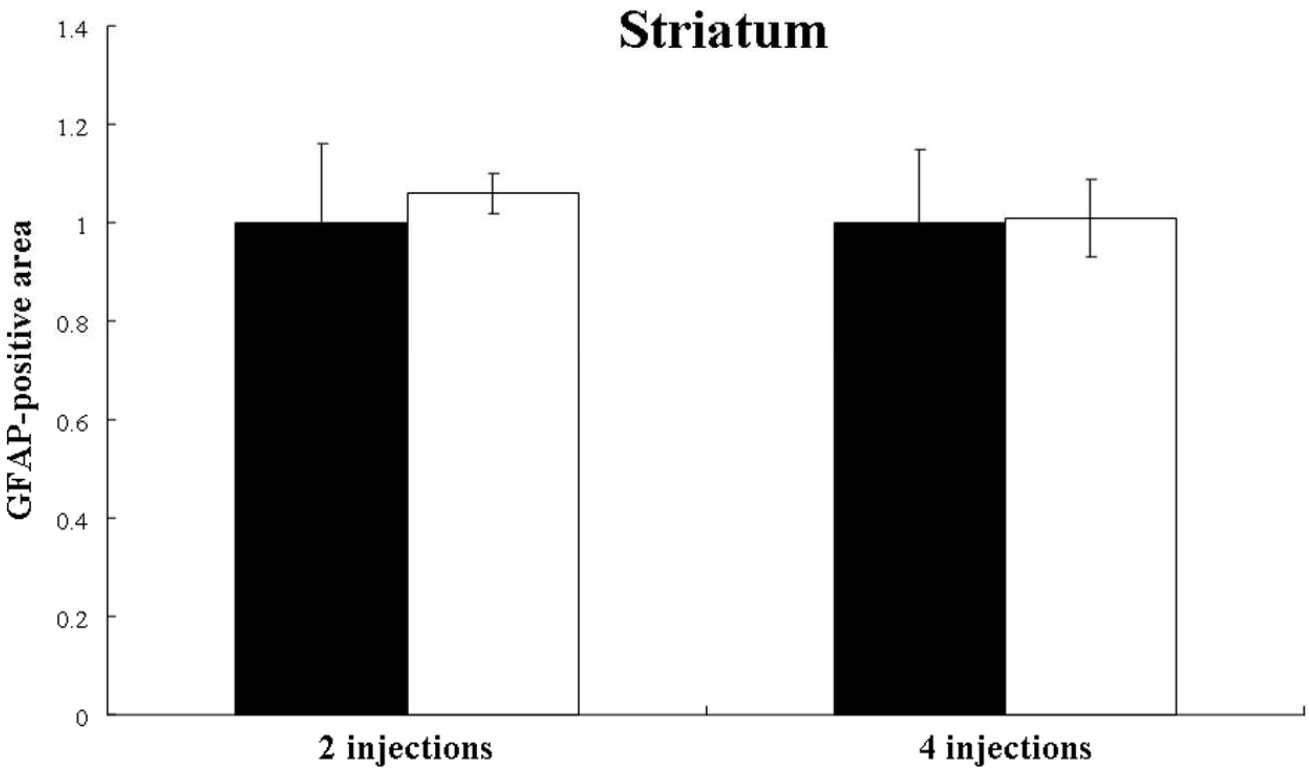

Figure 1-3. Results of quantitative analysis of GFAP-positive areas in the striatum. GFAP-positive areas are represented as the mean ± SD (n = 3). No significant differences are observed between MPTP-treated GH (□) and controls (■).

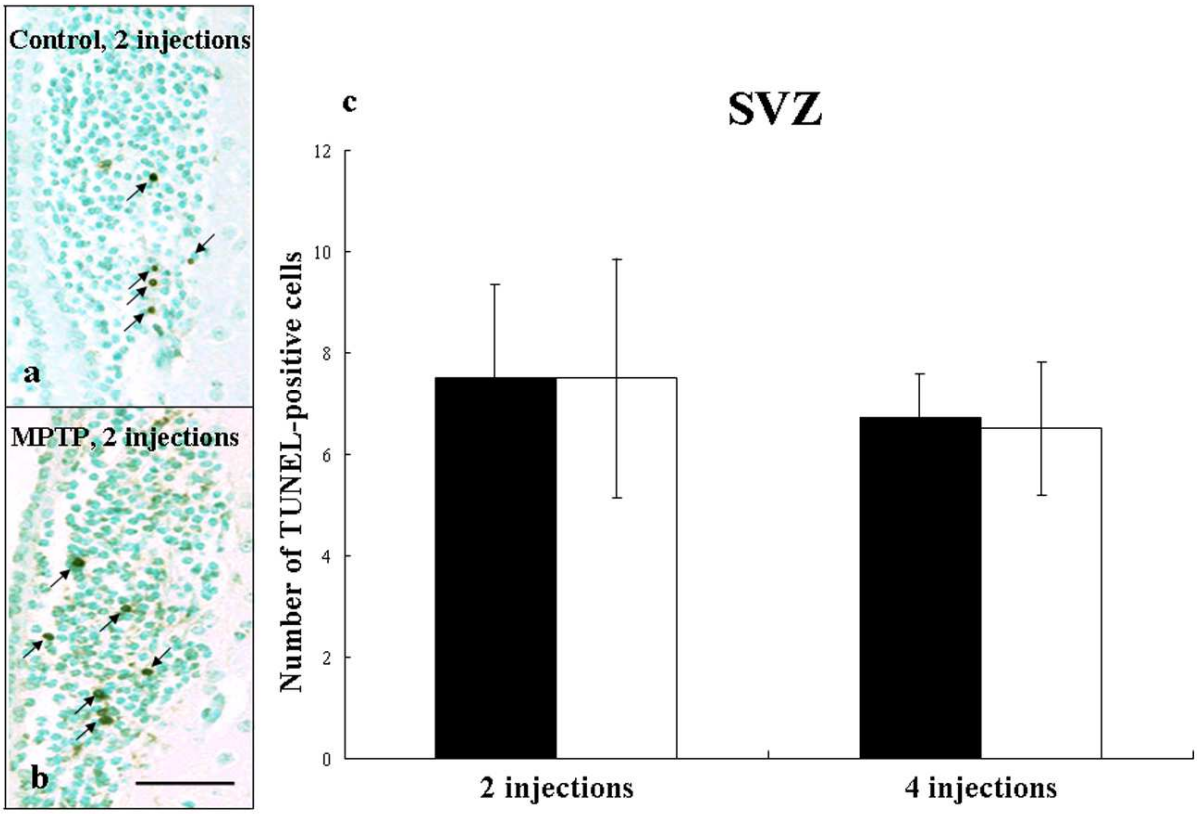

Figure 1-4. Detection of apoptotic cells in the SVZ of control (**a**) and MPTP-treated GH (**b**) after an acute ip treatment. Arrows are indicating TUNEL-positive cells. Bar = 150 µm. Figure **c** shows the quantitative analysis for TUNEL-positive cells. No statistical differences are observed between MPTP-treated groups and their respective controls. ■ = control; □ = MPTP.

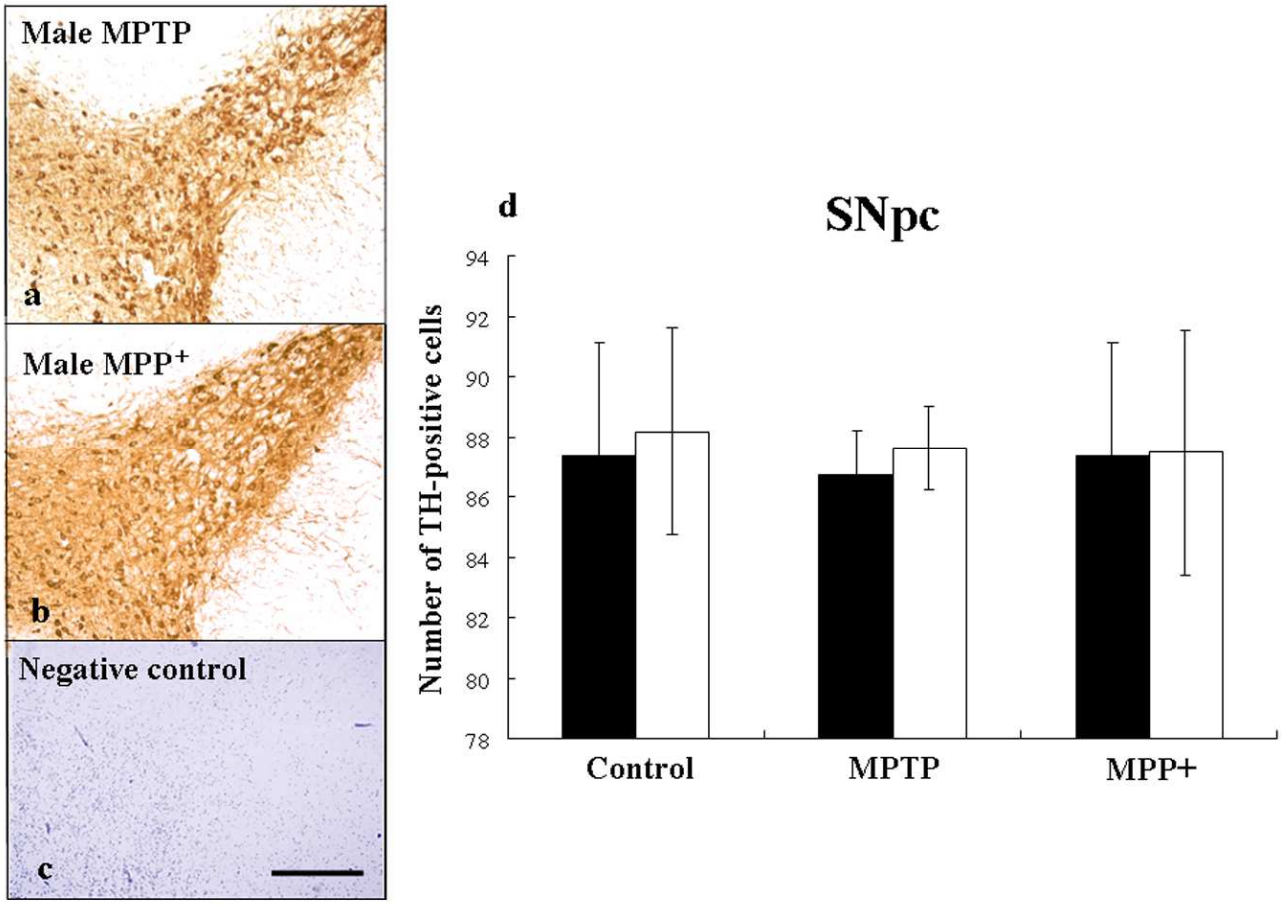

Figure 1-5. Results of TH-immunostaining in the SNpc after MPTP or MPP^+ icv administration (**a** and **b**) and photomicrograph of a negative control (**c**) to show the lack of TH-unspecific binding. Bar = 300 μm. Figure **d** shows the quantitative analysis of TH-positive cells, which are represented as the mean±SD (n = 7). No significant differences are observed between groups. ■ = female; □ = male.

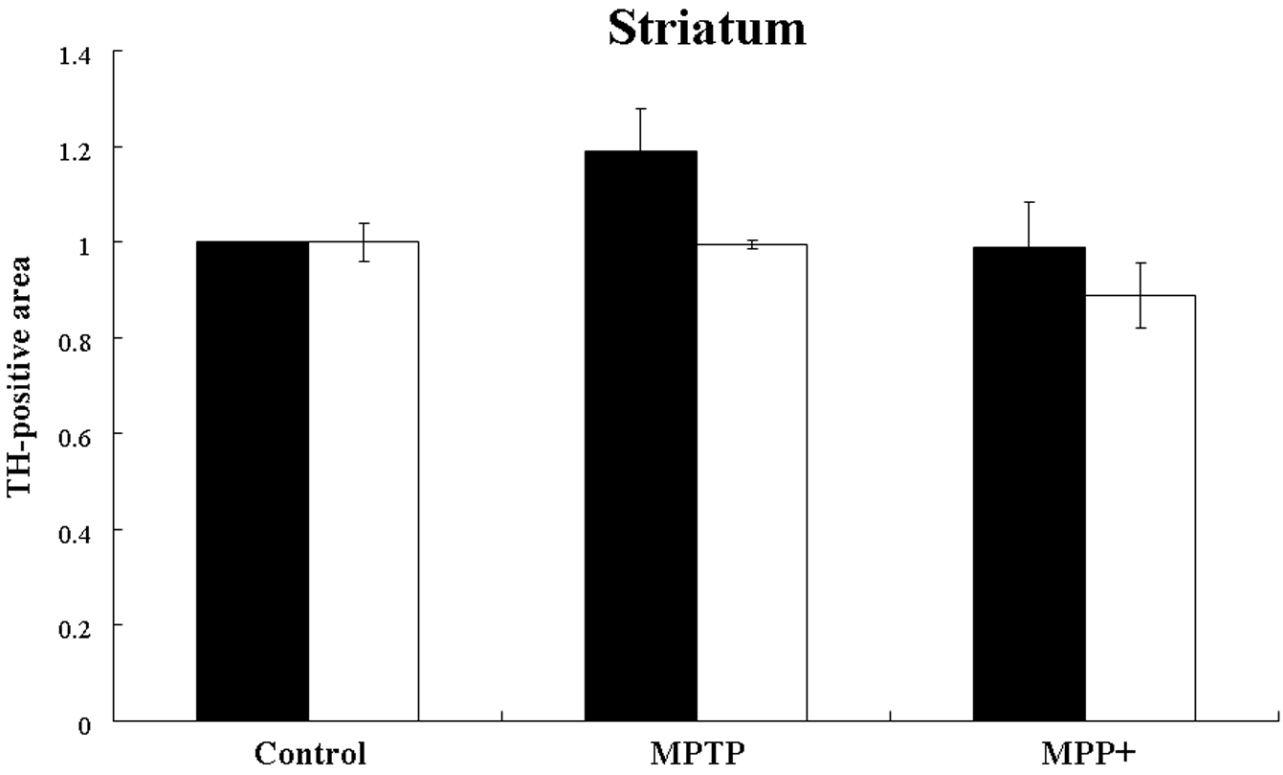

Figure 1-6. Results of quantitative analysis of TH-positive areas in the striatum after MPTP or MPP^+ icv administration. TH-positive areas are represented as the mean±SD (n = 3). No significant differences are observed between groups. ■ = female; □ = male.

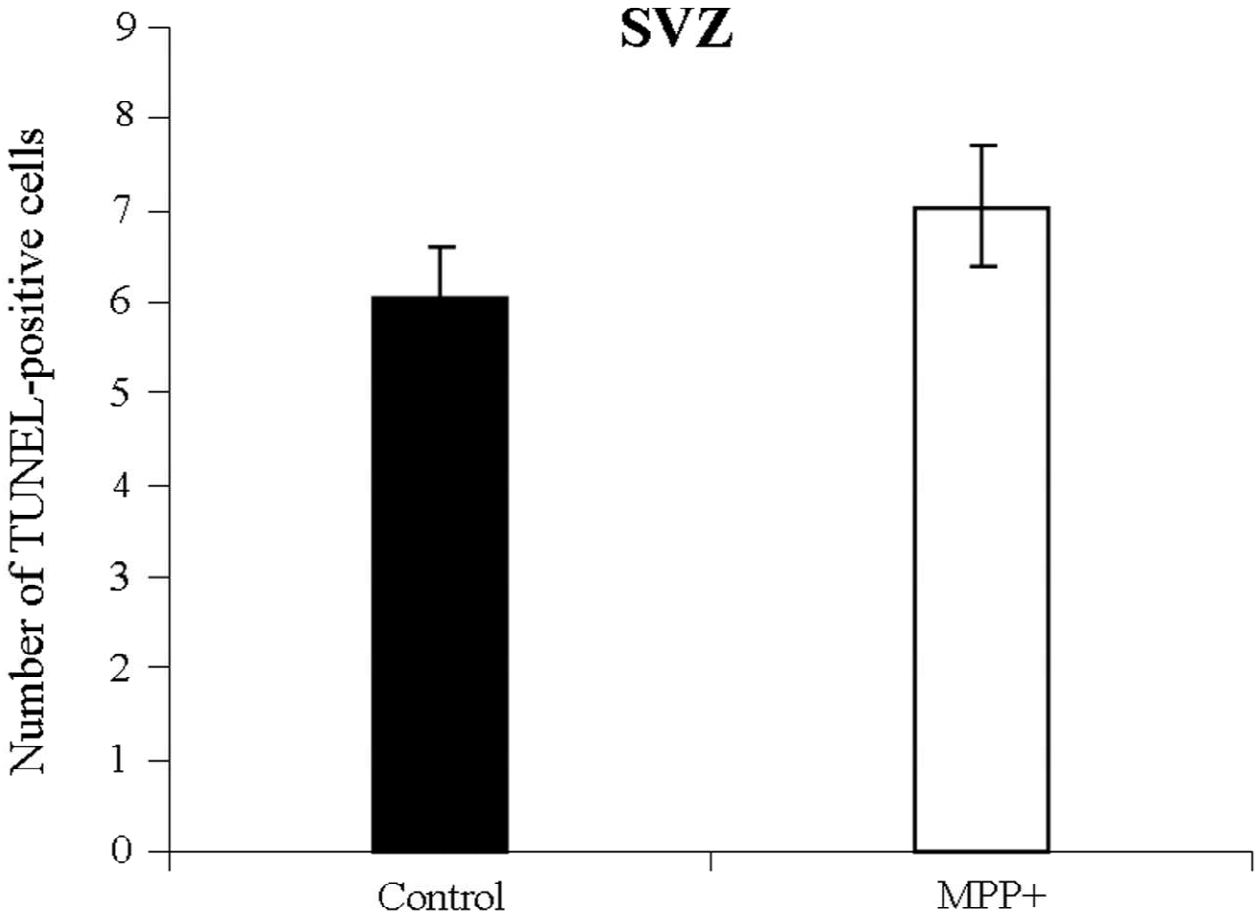

Figure 1-7. Results of quantitative analysis of apoptotic cells in the SVZ one day after MPP^+ icv administration. No significant differences are observed between the MPP^+-treated group and control.

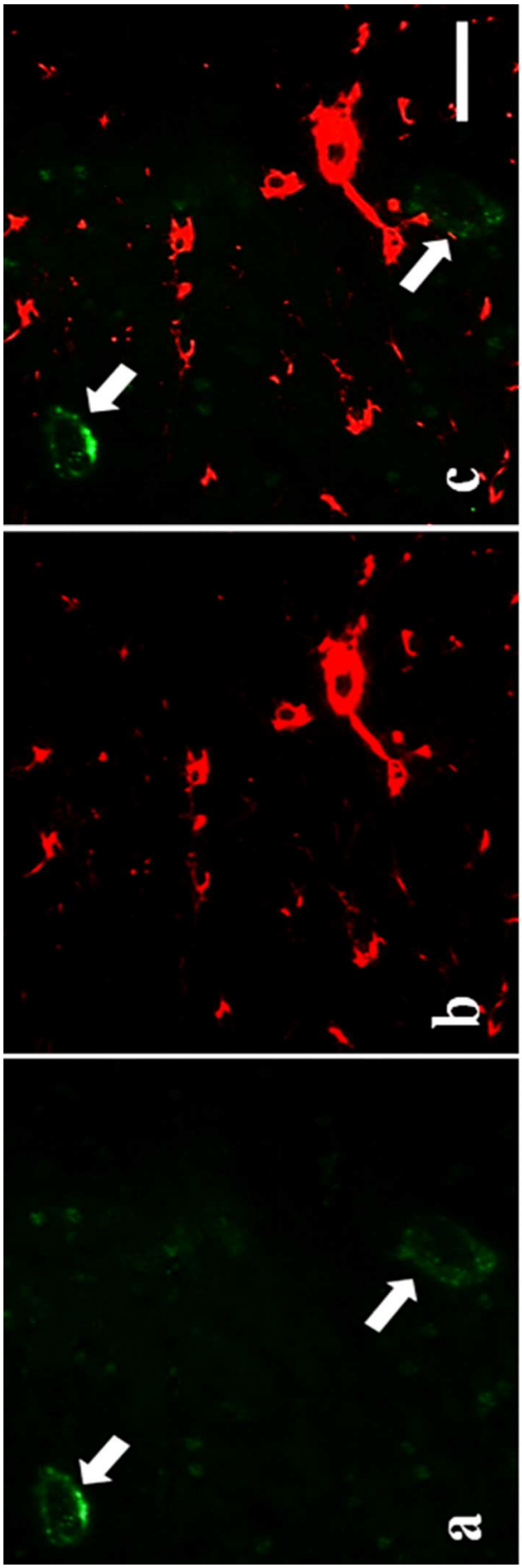

Figure 1-8. Results of immunofluorescence for MAO-B (**a**, green) and GFAP-positive astroglia (**b**, red). Micrograph **c** is the merge of **a** and **b**. Arrows are showing capillaries. The lack of coexistence between MAO-B and GFAP indicates that the enzyme is not in the astrocytes. Bar = 20 µm.

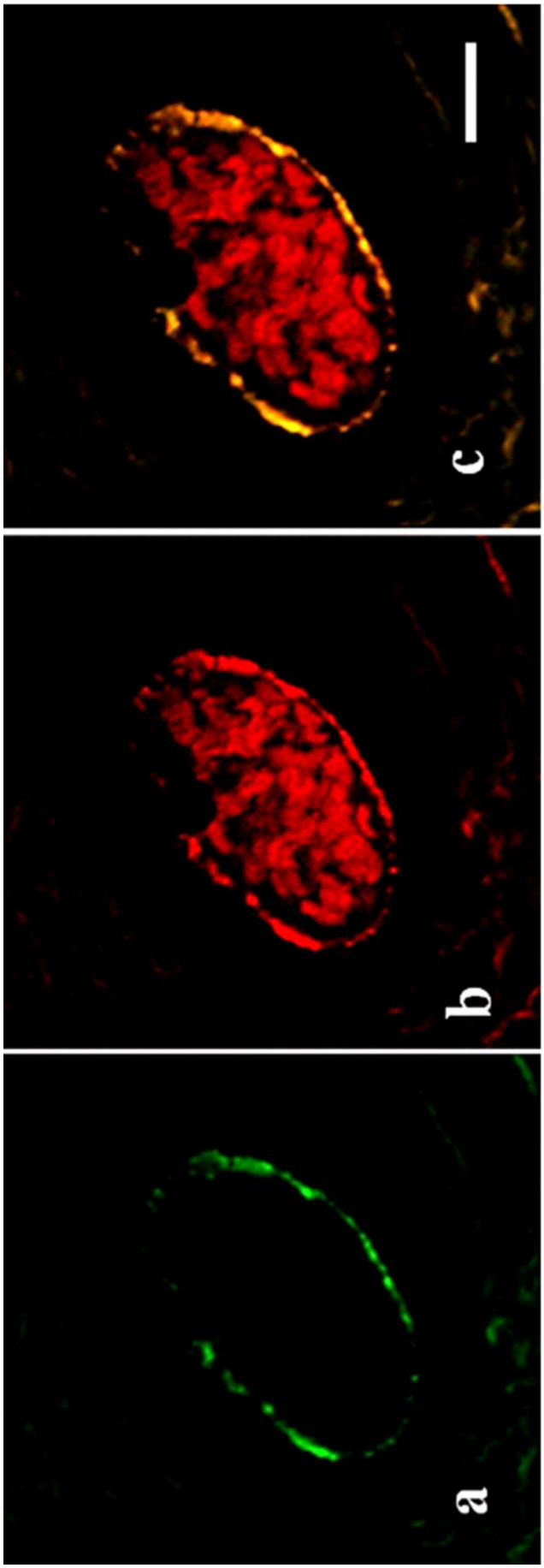

Figure 1-9. Results of immunofluorescence for MAO-B (**a**, green) and CD-31 (**b**, red). Micrograph **c** is the merge of **a** and **b**. The coexistence of MAO-B and CD-31 indicates that the enzyme resides predominantly in the endothelial cells. Erythrocytes in the vessel (**b** and **c**) correspond to a non-specific immunostaining. Bar = 40 µm.

Chapter 2

Immunohistochemical changes of nigrostriatal TH and DAT in the GH after a single intrastriatal injection of 6-OHDA

Abstract

One of the most important models for analyzing the pathomorphological aspects of PD is the 6-OHDA model where lesions of the nigrostriatal axis are observed when 6-OHDA is intrastriatally injected.

Despite the widespread use in rats, only few studies have explored the toxicity of 6-OHDA in other species. In the present chapter, I evaluated the effects of a single intrastriatal injection of 6-OHDA in the young-adult GH. Significant decreases in the TH- and DAT-positive areas were found in the ipsilateral striatum at day 3 after the injection. On the other hand, no effect of injection was found on the contralateral side. In the SNpc, a significant decrease in the number of TH-positive cells appeared one week after the injection with the peak in the loss of TH-positive immunoreactivity being recorded two weeks post-injection. These results show that GH is highly-sensitive to the effects of 6-OHDA-induced neurotoxicity.

Introduction

The single intrastriatal administration of 6-OHDA in rats induces a direct toxic damage of dopamine axons as early as 24 hours after the injection, followed by a loss of dopamine neurons localized in the SNpc ipsilateral to the injection [19-22, 62-64], while the two-site injection of 6-OHDA in ganglionectomized Sprague-Dawley rats induces a nearly complete lack of TH-immunopositive fibers in the striatum and TH-positive neurons in the SNpc ipsilateral to the injections [18]. To date, no reports of the sensitivity of the GH to 6-OHDA have been available

The present chapter provides an immunohistochemical characterization and a time course progression of the nigrostriatal TH and DAT loss in the 6-OHDA-injured GH.

Materials and methods

Animals

Young adults (10- to12-week old) male GHs (*Mesocricetus auratus*) (SLC, Tokyo, Japan) weighing 100 to 120 g were used in the present study. GHs were housed individually in a temperature-controlled room (23 ± 2 °C) with a constant level of humidity (55 ± 5%) under a 12/12 h light/dark cycle and free access to food and water. The procedures used in the present study were examined and approved by the Committee of Animal Experiments, Graduate School of Agricultural and Life Science, the University of Tokyo. All the efforts were made in order to reduce the number of animals and their suffering.

Intrastriatal injection of 6-OHDA

The animals were anesthetized with 4% chloral hydrate (MYLAN, Osaka, Japan) using a dose of 360 mg/kg and then placed into a stereotaxic frame (Narishige SR-5M, Narishige, Tokyo, Japan). The procedures were performed as follows: after exposing the skull, one hole was drilled in the right side using the following coordinates with respect to the bregma: AP:＋1.5; ML: 2.1; DV: -5.0. Using a Hamilton-10μl-syringe (Hamilton,

Reno, Nevada, USA) with a 26-gauge-blunt-type needle, 2 µl of vehicle (2% ascorbic acid dissolved in 9% NaCl solution) or 20 µg of 6-OHDA (Sigma, St. Louis, MO) dissolved in 2 µl of vehicle (reaching to a final dose of approximately 0.03 mg/kg) were injected once with an electric micromanipulator (SM-15, Narishige, Tokyo, Japan) at a rate of 0.5 µl/min. After the injection, the needle was left in the place for 6 min and then gradually withdrawn. The place was cleaned and the incision was closed using Michel wound clips (Kent scientific corporation, Washington, DC). To avoid the hypothermia due to the anesthesia, the animals were placed in a heated box and kept there until their complete recovery. In order to avoid the degradation of the 6-OHDA, the solution was freshly prepared and kept in a dark box at 4°C until its utilization. Animals included in the experiments completed the observation period without postsurgical complications.

Experimental design

Animals were split into five groups, according to the days (d) of sacrifice after the intrastriatal injection, as follows: 3 d (n=3), 5 d (n=3), 7 d (n=4), 15 d (n=7) and 21 d (n=4). For each treated group there was a comparable control injected only with a vehicle solution.

Tissue preparation

All the animals were euthanized by a cervical dislocation after being deeply sedated with diethyl ether. All the procedures employed for the recollection of the brains were performed following the recommendations made by the American Veterinary Medical Association (AVMA) in the "Guidelines on Euthanasia" (http://www.avma.org/issues/animal_welfare/euthanasia.pdf). Once localized, the brain was exteriorized by removing the calvarium and, using a blunt spatula, removed, isolated and immediately fixed in 10% neutral buffered formalin. Brain tissues were embedded in paraffin by a routine procedure and then sliced into 4 µm coronal sections encompassing the complete striatum and SNpc.

Immunohistochemistry

Paraffin sections were used for immunohistochemistry with the following primary antibodies: rabbit anti-TH (1:400; Millipore, Temecula, CA) and rabbit anti-DAT (1:100; Novus Biologicals, Littleton, CO). After deparaffinized, the sections were subjected to a heat-induced epitope unmasking in 10 nM citrate buffer (pH 6.0) in autoclave at 121 °C for 10 min, then treated with 10% hydrogen peroxide/methanol for

5 min to inactivate endogeneous peroxidase and incubated in 8 % skim milk/TBS at 38 °C for 40 min to block non-specific binding of the antibodies. Tissue sections were then incubated at 4 °C overnight with the first antibodies diluted in TBS, and then developed using the anti-rabbit HRP Envision System (DAKO, Carpinteria, CA) at 37 °C for 60 min. Finally, the reaction products were visualized in a 0.05% 3,3´-diaminobenzidine (DAB) solution with 0.03% hydrogen peroxide in Tris–HCl buffer followed by conterstaining with 5 % methyl green (pH 4.0).

Measurements and statics

Serial brain coronal tissue specimens were obtained according to “A stereotaxic atlas of the golden hamster brain” [36]. At least 5 specimens in the SNpc and 8 specimens in the striatum per animal were blindly applied for quantitative analyses.

Cells (SNpc) and positive areas (striatum) were quantified using Image J software (http://rsb.info.nih.gov/ij/). The procedures to quantify positive cells were performed as follows: once stained, tissue sections were viewed with an Olympus BX50 microscope (magnification x10) and one picture per specimen was taken using a Nikon DXM1200F digital camera. The images were then converted to grayscale binary image (8 bit) and a

limit of threshold was adjusted in order to select only cells with a size > 600 pixel^2 and circularity between 0.1 and 1.0. After founding the optimal threshold, the cells were counted using the function “Analyze Particles”. In the striatum, non-overlapping digital photomicrographs from both hemispheres (ipsilateral and contralateral striatum) were captured using a Nikon COOLSCAN IV ED (LS-40 ED) digital scanner with a magnification of x8. Eight sequential photomicrographs per animal, extending approximately from +2.5 mm to -0.5 mm with respect to the bregma, were obtained. The images were then converted to grayscale binary image (8 bit) and the limit to threshold area function within Image J software was used to calculate a semi-quantitative index of the relative areas of each antibody. For statistical purposes, control group was given a relative value of 1 and the results in the treated group are expressed as relative values with respect to that of the control group. One-way ANOVA test was performed to assess potential differences between control and treated groups. Differences were considered statistically significant when $p < 0.05$. The normal distribution for each group of animals was checked using a normal probability plot and the homogeneity of variance was checked using *f*-test for two samples.

Results

Clinical symptoms

Despite abnormal posture, there were no typical Parkinsonian motor abnormalities such as bradykinesia, muscular rigidity or tremor in the animals injected with 6-OHDA.

6-OHDA induces a marked reduction in the striatal TH-immunopositive fibers (Fig. 2-1)

In the ipsilateral striatum, I found a markedly reduced striatal TH-positive area by up to 62%, 84% and 83% at days 3, 5 and 7 post injection, respectively ($p < 0.01$). Interestingly, the TH-immunoreactivity in the ipsilateral striatum of the animals sampled at days 15 and 21 post injection tended to be slightly higher than those observed at days 5 and 7 post injection. On the other hand, the contralateral hemisphere showed no significant changes between control and treated groups.

6-OHDA induces a marked decrease of TH-immunopositive neurons in the SNpc (Fig. 2-2)

In the ipsilateral SNpc, I found a markedly reduction of TH-positive cells by up to 31.8%, 75.1% and 72.2% in the groups sampled at days 7, 15 and 21 post injection,

respectively ($p < 0.01$). The contralateral hemisphere showed no significant changes between control and treated groups.

With regard to the pathomorphological aspects of the TH-positive remaining cells in the ipsilateral SNpc of the treated animals, most of the cells were shrunk and rounded with condensed-small nuclei **(Fig. 2-3)**.I also detected that the first cells to disappear were those next to the medial terminal nucleus of the accessory optic tract, which may indicate that the cell loss progresses caudo-rostrally in the SN.

6-OHDA induces a marked reduction in the striatal DAT-immunopositive fibers (Fig. 2-4)

In the ipsilateral striatum, I found a markedly reduced striatal DAT-positive area by up to 61%, 88% and 92% at days 3, 5 and 7 post injection, respectively ($p < 0.01$). The DAT-immunoreactivity at days 15 and 21 post injection tended to be slightly higher than those observed at 5 and 7 days.

DAT expression in the SNpc (Fig. 2-5)

DAT expression in the midbrain of control animals revealed that positive cells are localized mainly in the SNpc and very few of them are observed in the substantia nigra

reticular (SNR). There was a weak immunoreactivity in treated animals sampled at days 3 and 5 post injection, and the specimens sampled at days 7, 15 and 21 post injection showed a complete lack of DAT-positive cells in the ipsilateral SNpc.

Discussion

Based on the data presented herein, I can conclude that, when injected into the striatum, 6-OHDA depletes TH-positive DA neurons in the nigrostriatal axis of the GH. Neurotoxic effects of 6-OHDA upon nigrostriatal cells in the rat and mouse have been fully described [17-24]. The results presented in this chapter extends these observations by using a one-site intrastriatal protocol and focuses on the time-course of the histopathological damages in the nigrostriatal axis of the GH. A single intrastriatal injection of 6-OHDA induces significant decreases in the ipsilateral striatal TH- and DAT-immunoreactivity as early as 3 days after the treatment, with the peak-decrease recorded at the first week and significant reductions in the number of TH-positive cells in the ipsilateral SNpc at one week after the injection. These results differ from previous reports in the 6-OHDA rat model, where the peak-decrease in the loss of dopaminergic terminals was observed at three weeks after a single intrastriatal injection [22, 65] and the loss of TH-positive cells took place in a period of four to eight weeks [20]. Ichitani et al. [19] have proposed two different mechanisms to explain the retrograde effects of 6-OHDA: i) a retrograde axonal transport of 6-OHDA or some metabolites produced in

the striatal terminals, which implies that changes of the neuronal perikarya in the SNpc may begin shortly after the striatal injection and ii) a direct damage upon striatal terminals followed by a slow retrograde degeneration of neuronal perykarya in the SNpc. With regard to this last mechanism, some studies have shown that neurons in the SNpc undergo retrograde degeneration as a consequence of the lack of trophic support [66-68] and that the slow nigral cell loss observed in the rat after an intrastriatal injection of 6-OHDA could be explained due to the lack of some trophic stimulus [20]. Hence, although I can not rule out the possibility of a retrograde degeneration leading to cell death in the SNpc in the GH model, I speculate that the changes of the nigral cells, that tend to appear faster than in the rat, could be explained due to the predominance of a retrograde transport of 6-OHDA or some of its metabolites.

It is believed that the uptake of 6-OHDA into catecholamine neurons is through specific carriers, such as DAT, which is an exclusive transporter for dopaminergic cells [69]. The data generated herein show that DAT and TH have a similar immunohistochemical distribution pattern in the striatum of the GH. These results correspond with previous studies in the rat [70-71], where the highest levels of DAT

were reported in the striatum, and suggest that DAT-positive axons and nerve terminals in the striatum of the GH are the functional site for the uptake of 6-OHDA.

Despite no significant differences in the TH- and DAT-relative areas in the ipsilateral striatum of treated animals, the specimens sampled at days 15 and 21 post injection seem to present a slightly higher immunoreactivity, which may be suggestive of recovery of dopamine fibers. Previous reports regarding the MPTP neurotoxicity have described a potential axonal recovery in mice [60, 72-74] and non-human primates [75]. The possibility of spontaneous recovery in the striatal dopaminergic system in MPTP-treated C57BL/6 young mice has been explained as a consequence of a regenerative sprouting from remaining intact fibers [76]. In the rat 6-OHDA model, it has been shown that the intranigral administration led to a sprouting of dopaminergic fibers in the ipsilateral striatum, although this partial recovery occurred from the fourth month and continued to the seventh month post lesion, but it was not recorded at 10 days post treatment [77-78]. Moreover, on the basis of some previous reports [79-80], I suggest that another possible explanation for the slightly higher immunoreactivity observed at days 15 and 21 post injection could be the up-regulation of TH biosynthesis

from the non-degenerative neurons in the nigrostriatal axis.

In conclusion, the results herein reported show that, unlike what happens with MPTP, the GH is sensitive to 6-OHDA. Due to its potential implications for treatment and prevention of neuronal injury or disease, the recovery of TH-immunopositive fibers will be discussed again in Chapter 4.

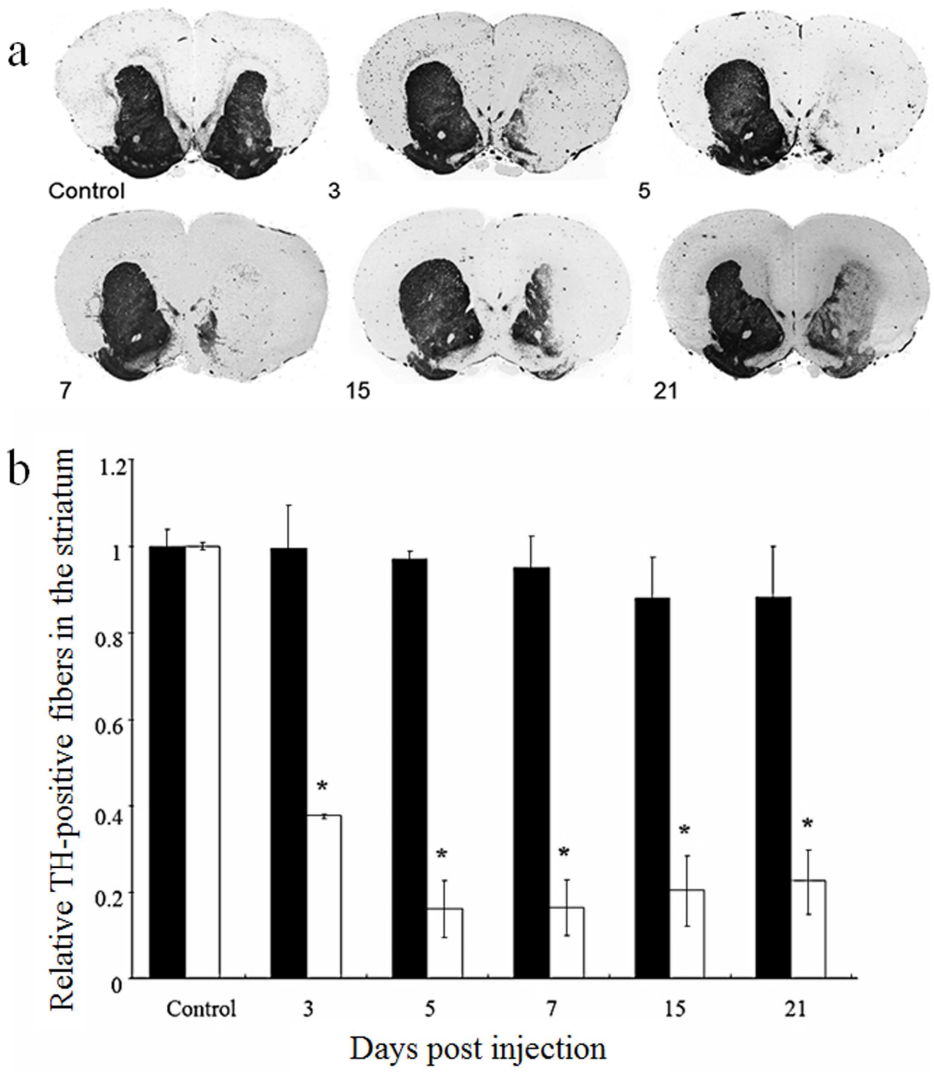

Figure 2-1. TH-positive fibers in the striatum. **a)** Cranial area of the striatum (+2.4 mm～+2.1 mm with respect to the bregma). The bottom numbers represent the day of sacrifice post injection. **b)** Results of the quantitative analysis of the relative TH-positive fibers in the striatum. Control group represents the average of each control group at different time points. ■ = contralateral striatum; □ = ipsilateral striatum. TH-positive fibers are expressed as the mean ± SD. $^{*}p < 0.05$; significantly different from the control group (One-way ANOVA test).

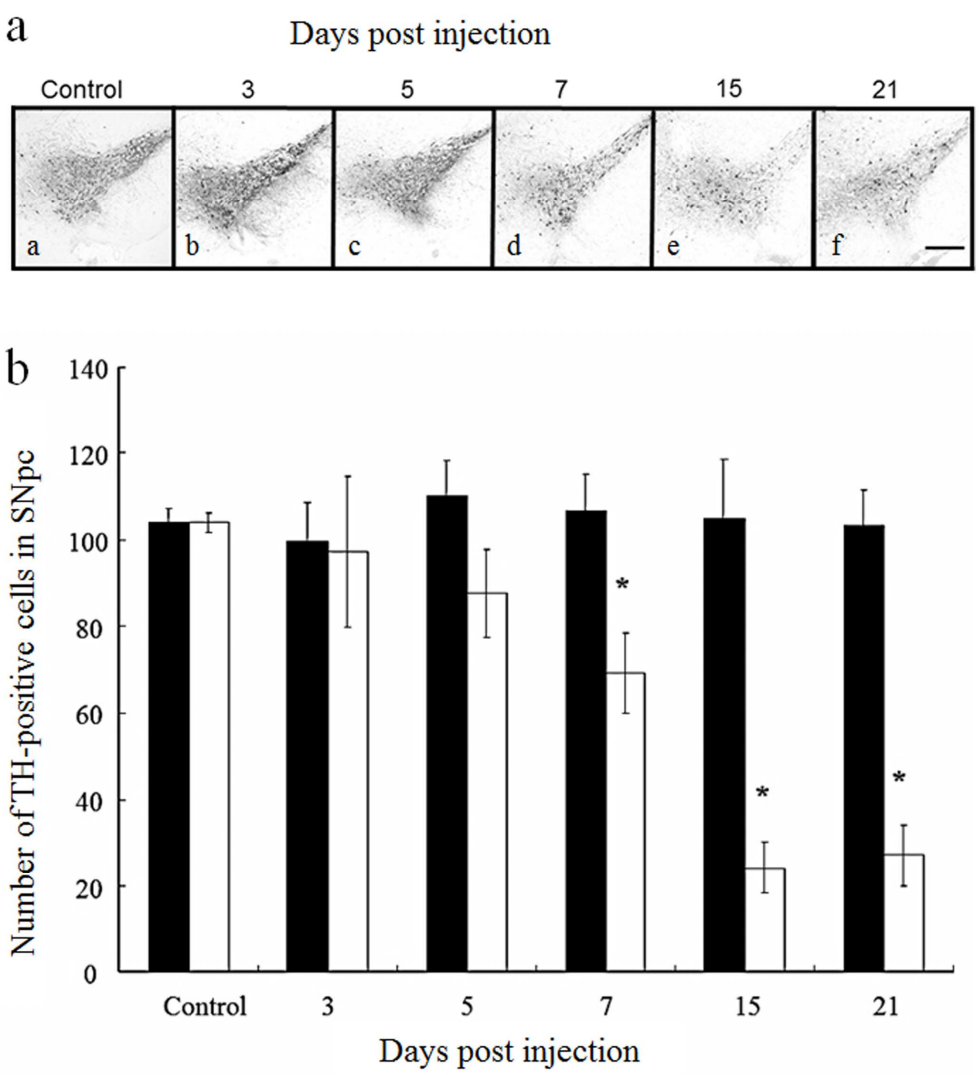

Figure 2-2. Number of TH-positive cells in the SNpc. **a)** Representative photomicrographs of coronal sections which show an intense loss of TH-positive cells at days 15 and 21 post injection. Scale bar = 200 µm. **b)** Quantitative analysis of the number of TH-positive cells in the SNpc. Control group represents the average of each control group at different time points. ■ = contralateral SNpc; □ = ipsilateral SNpc. The number of TH-positive cells is expressed as the mean ± SD. $^{*}p < 0.05$; significantly different from the control group (One-way ANOVA test).

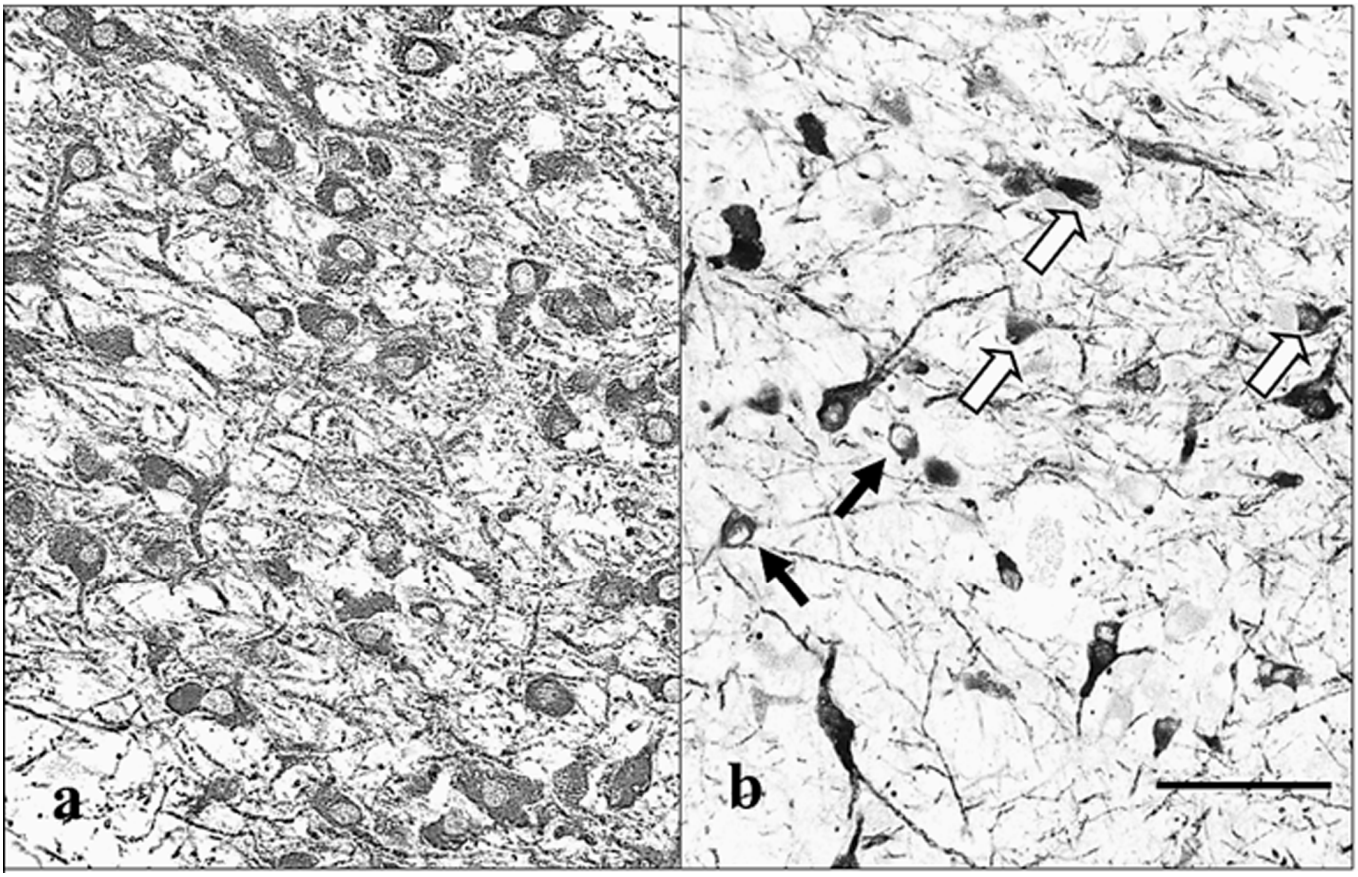

Figure 2-3. Representative photomicrographs of TH-positive cells in the SNpc of control **(a)** and 21-day sampled GH **(b)** to observe the pathomorphological changes in the TH-positive remaining cells. Note the presence of rounded (black arrows) and shrunk (white arrows) cells in the treated animal. All the remaining cells in the treated SNpc show condensed-small nuclei. Scale bar = 100 µm.

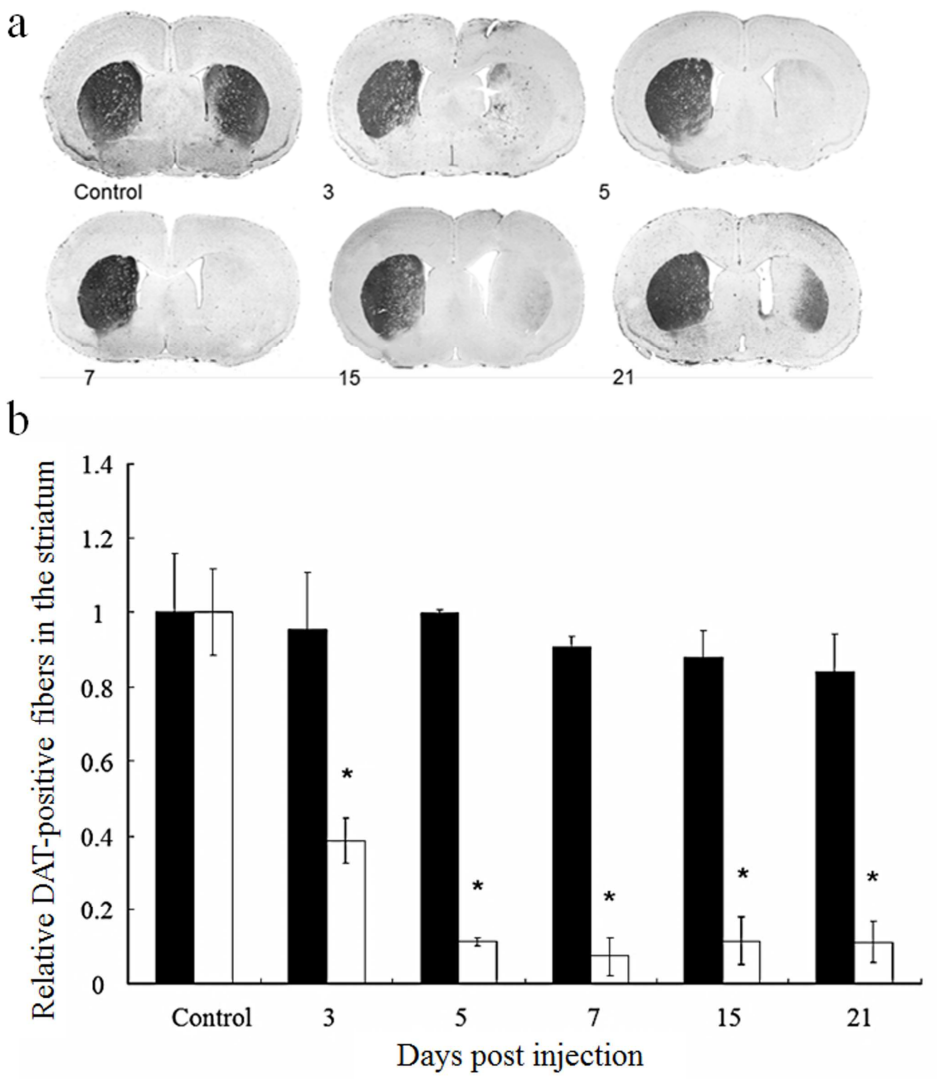

Figure 2-4. DAT-positive area in the striatum. **a)** Cranial area of the striatum (+1.2 mm with respect to the bregma). The bottom numbers represent the day of sacrifice post injection. **b)** Quantitative analysis of the relative DAT-positive area. Control group represents the average of each control group at different time points. ■ = contralateral striatum; □ = ipsilateral striatum. DAT-positive fibers are expressed as the mean ± SD. $^{*}p < 0.05$; significantly different from the control group (One-way ANOVA test).

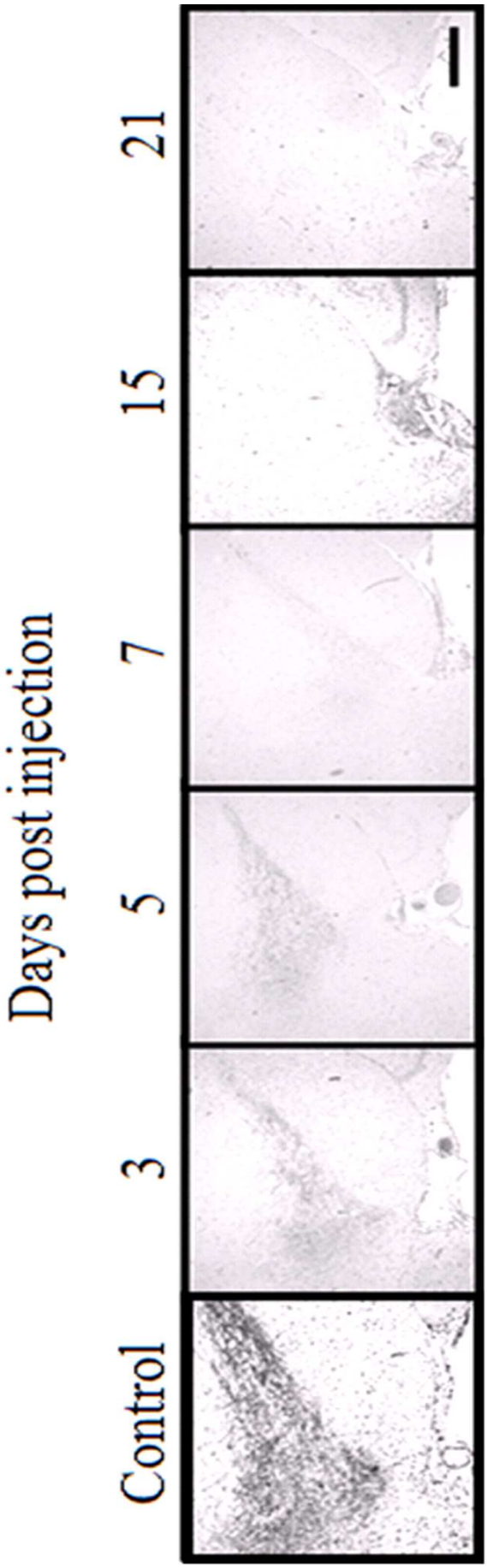

Figure 2-5. DAT-positive cells in the ipsilateral SNpc. The top numbers represent the day of sacrifice post injection. Note the weak or the lack of immunoreactivity in the treated GH sampled at days 3 to 21 post injection. Scale bar = 200µm.

Chapter 3

Histopathologic characterization of the brain lesions in the 6-OHDA-lesioned GH

Abstract

In the previous chapter, I evaluated the effects of a single intrastriatal injection of 6-OHDA on the nigrostriatal axis of the young-adult GH. In the present chapter, I examined whether apoptosis occurs in the SNpc and the histopathology of the lesions induced by a single intrastriatal injection of 6-OHDA. No apoptotic cells were present in the SNpc of 6-OHDA-injured GH at any time point analyzed, whereas in the striatum a few TUNEL-positive bodies were found in and around the site of injection.

The H&E stain revealed marked microglial activation in the ipsilateral striatum and SNpc by 6 hours and 3 days post-injury, respectively. Inflammatory cells were identified by immunohistochemistry using antibodies against Iba-1, CD3 and myeloperoxidase. Only Iba-1-immunopositive cells (macrophages) were found in the nigrostriatal axis. In addition, GFAP-immunostaining revealed widespread reactive astrocytosis by 5 days after injury.

The results of this chapter show that 6-OHDA triggers a rapid immune response characterized by microglia/macrophages recruitment and astrocytosis. In addition, they suggest that apoptosis is not the principal cell-death mechanisms triggered by 6-OHDA.

Introduction

6-OHDA is believed to selectively induced nigrostriatal dopaminergic cell degeneration [81], but the mechanisms by which cell injury finally leads to dopaminergic cell death remain still unclear. Although it has been suggested that apoptosis may play a role in PD, some post-mortem studies failed to show apoptotic cell-death in the nigrostriatal axis of human with sporadic PD [82-83].

In the present chapter, I examined whether 6-OHDA-induced neurotoxicity triggers cell-death via apoptotic mechanisms. In addition, I studied the non-specific lesions and the cell recruitment induced by 6-OHDA in the GH PD model introduced in Chapter 2.

Material and methods

Animals

Twenty-one 10- to12-week-old male GHs (*Mesocricetus auratus*) (SLC, Tokyo, Japan) weighing 90 to 120 g at purchased were used in this study. Animals were housed individually in a temperature-controlled (23 ± 2 °C) room with a constant level of humidity (55 ± 5%) under a 12/12 h light/dark cycle and free access to food and water. The procedures used in the present study were approved by the Committee of Animal Experiments, Graduate School of Agricultural and Life Science, the University of Tokyo. All the efforts were made in order to reduce the number of animals and their suffering.

Intrastriatal injection of 6-OHDA

Intrastriatal injection of 6-OHDA was performed as described in **Chapter 2**. For details, see Materials and methods; Intrastriatal injection of 6-OHDA; page 36.

Experimental design

According to the hours (h) or days (d) of sacrifice after intrastriatal injection, animals were split into seven groups, as follows: 6 h, 12 h, 24 h, 3 d, 5 d, 7 d and 15 d. One animal per group was intrastriatally injected with vehicle solution to serve as control.

Tissue preparation

Animals were euthanized by cervical dislocation after being deeply anesthetized with diethyl ether. The brain was exteriorized by removing the calvarium, removed and fixed in a 10% neutral-buffered formalin solution. After 48h fixation, 4-µm-thick paraffin sections, encompassing the complete striatum and SNpc, were sliced and subsequently used for TUNEL staining, immunohistochemistry and immunofluorescence histochemistry, as well as for staining with hematoxylin and eosin (H&E).

TUNEL method

Tissue sections were processed for TUNEL staining by using the ApopTag peroxidase In Situ Apoptosis Detection Kit (Chemicon, Temecula, CA), according to the manufacturer's instructions. Negative controls were processed in parallel with the use of saline solution instead of Tdt enzyme. Tissue sections were finally counterstained with 5% methyl green solution pH 4.0.

Immunohistochemistry

Paraffin sections were used for immunohistochemistry with the following primary antibodies: i) rabbit anti-Iba1 (1:500, Wako Pure Chemical Industries, Osaka, Japan) as

a marker of microglia; ii) rabbit anti-CD3 (1:50; DAKO, Carpinteria, CA) as a marker for T lymphocytes; iii) rabbit-anti myeloperoxidase (1:300; DAKO, Carpinteria, CA) as a marker for neutrophils; and iv) rabbit anti-GFAP (1:500; DAKO, Carpinteria, CA) as a marker for astrocytes.

For antigen retrieval, deparaffinized sections were autoclaved at 121°C for 15 min. Endogenous peroxidase activity was blocked by incubating the sections with 3% hydrogen peroxide in methanol at room temperature for 5 min. For blocking nonspecific reaction, the sections were further treated with skimmed milk at 37°C for 40 min. The sections were then incubated at 37°C for 1 h with the primary antibodies. Thereafter, the sections were incubated with the Envision polymer reagent (DAKO Japan, Kyoto, Japan) at room temperature for 40 min and then visualized using 0.05% 3,3-diaminobenzidine (DAB) with 0.03% hydrogen peroxide in Tris–HCl buffer, before being counter-stained for 45 sec with hematoxylin.

Results

Apoptosis

TUNEL-positive cells in the ipsilateral SNpc were conspicuously absent at any of the time points analyzed **(Fig. 3-1, right panels)**.

In the ipsilateral striatum, a few TUNEL-positive cells in the site of injection were detected by 6 h after injury **(Fig. 3-1, left panels)**. By 3 days, most of the samples analyzed showed no trace of apoptotic bodies in the ipsilateral striatum.

Microglial cells

Using H&E stain, by 6 h post-injection, I found a malacic area surrounded by few "reactive" inflammatory cells in the ipsilateral striatum of 6-OHDA-injected GH. Reactive cells increased in number greatly so that they dominated the lesion in five days. Thereafter, their number decreased slowly **(Fig. 3-2)**. In the SNpc, inflammatory cells were detected from day 3. The vehicle injection in control animals produced a limited non-specific damage of the striatal tissue. By day 5, only few remaining cells adjacent to the track of the needle were observed **(Fig. 3-2.c)**. No inflammatory cells were detected in the SNpc of animals injected with saline solution.

Analysis by immunohistochemistry showed that the reactive cells in the injured area stained for Iba-1. The Iba-1-immunopositive cells that first migrated at the margin of the injury site (6 h post-injection) exhibited short and thick processes and a rounded appearance as the cytoplasmic volume was increased **(Fig. 3-3)**. By day 5, Iba-1-immunopositive cells in the ipsilateral striatum exhibited pale cytoplasm and no definite processes **(Fig. 3-4.a)**. Meanwhile, in the SNpc, Iba-1-immunopositive cells were firstly observed 3 days post-injection and they became clearly evident at day 5. Morphologically, these cells exhibited most of the characteristics of the cells seen in the ipsilateral striatum 6 hours after the injection **(Fig. 3-4.b)**.

CD3- and myeloperoxidase-positive cells in the ipsilateral, injured striatum and SNpc of the 6-OHDA-injected GH were conspicuously absent at any of the time points analyzed.

Astroglial cells

Immunohistochemistry for GFAP antibody was used to identify whether astrogliosis occurs after 6-OHDA injection. By day 5, astroglial cells were evident in the nigrostriatal axis **(Fig. 3-5)**.

Discussion

In the current chapter, I described the histological changes associated with a single intrastriatal injection of 6-OHDA in the hemiparkinsonian GH presented in Chapter 2.

Apoptosis was not observed in the ipsilateral SNpc at any time point. There are several possible explanations for the absence of TUNEL-positive cells in the SNpc of 6-OHDA-injured GH. The most likely, perhaps, is that an alternate form of programmed cell death occurs in this area. It has been previously described that several cell morphologies may be observed during cell death and apoptosis is only one of these forms [33]. Since different signals probably trigger different types of cell-death, my results suggest that, in the GH, 6-OHDA triggers a morphological type of cell-death different from apoptosis. Meanwhile, the few TUNEL-positive bodies detected in the striatum may be the result of a direct insult induced by the mechanical injury associated with the injection and not a specific response to 6-OHDA.

A rapid, acute infiltration of microglia/macrophages (Iba-1-positive cells) occurred in the ipsilateral striatum within 6 hours after 6-OHDA injection and in the SNpc within the 3 days after injury. It is well known that microglial cells respond to immune insults

with a rapid morphological transformation into active ameboid cells [84]. This process is referred to as *activation of microglia* and it is associated with an enhanced expression of cytokines and growth factors [85-87].

It is noteworthy that while some reports described no astrocytic reaction in the SNpc of the rat intrastriatally injected with 6-OHDA [88], and in postmortem samples of patients with sporadic PD [89], I found a clear astrocytosis in the SNpc by 5 days post-injection. This later astrogliosis suggests that activated-microglial cells may release some trophic factors that stimulate astrocytes to proliferate. Hence, the appearance of numbers of macrophages and astrocytes following the induction of nigrostriatal lesion by 6-OHDA may have important implications which merit primary consideration. In this context, and taking into account that cells in the SNpc may be susceptible to microglia-mediated toxicity [90], the potential influence of microglial and astroglial cells in the onset and progression of the dopamine cell degeneration in the 6-OHDA-injured GH will be explored in the next chapter.

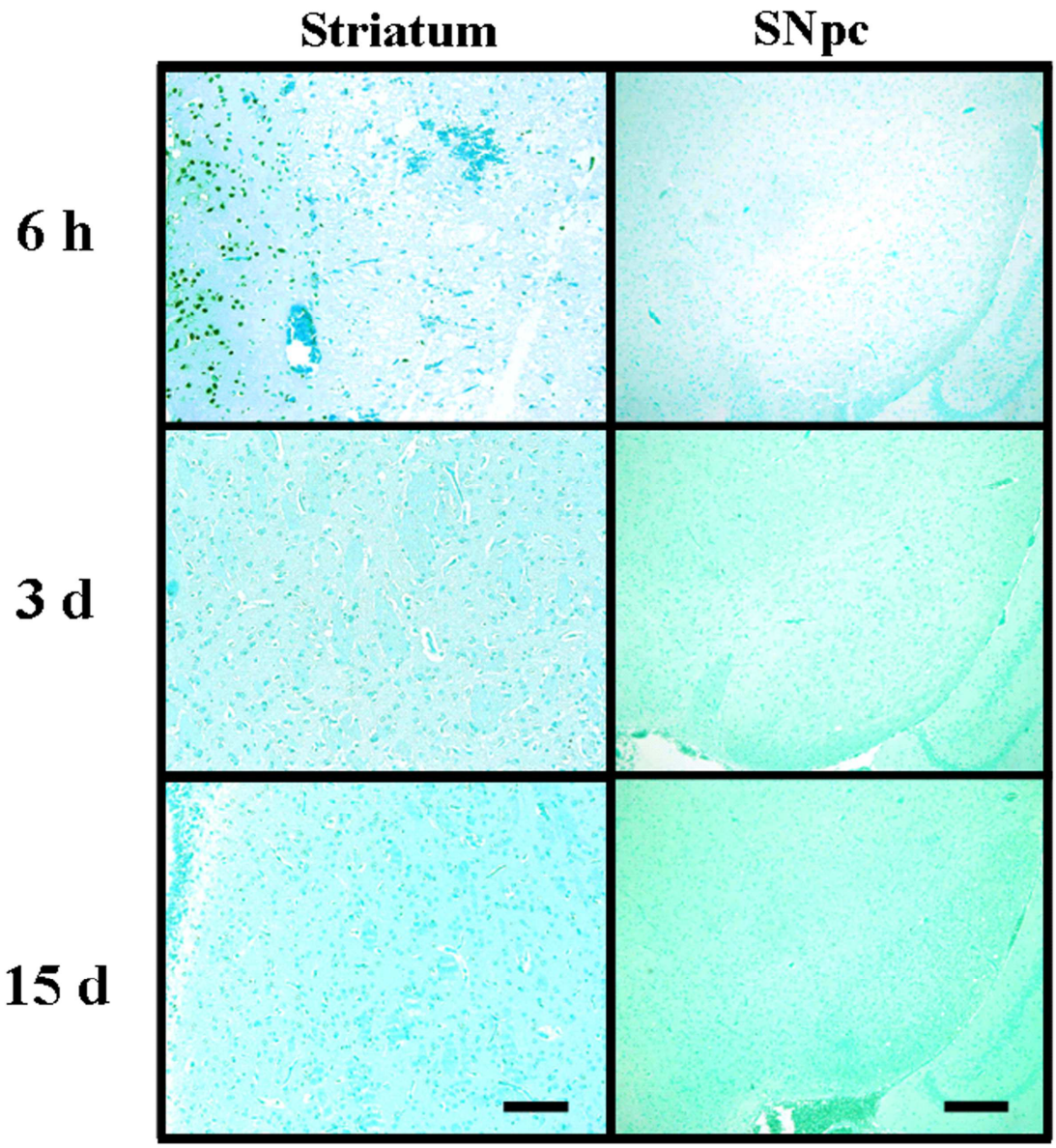

Figure 3-1. Detection of apoptotic cells at different time points. TUNEL-positive cells were conspicuously absent in the ipsilateral (right) SNpc at any time point. By 6 h post-injection, TUNEL-positive bodies in the ipsilateral (right) striatum were restricted to the site of injection. By 3 d post-injection, no TUNEL-positive bodies were found in the ipsilateral striatum. Scale bars = 100 µm (striatum) and 200 µm (SNpc).

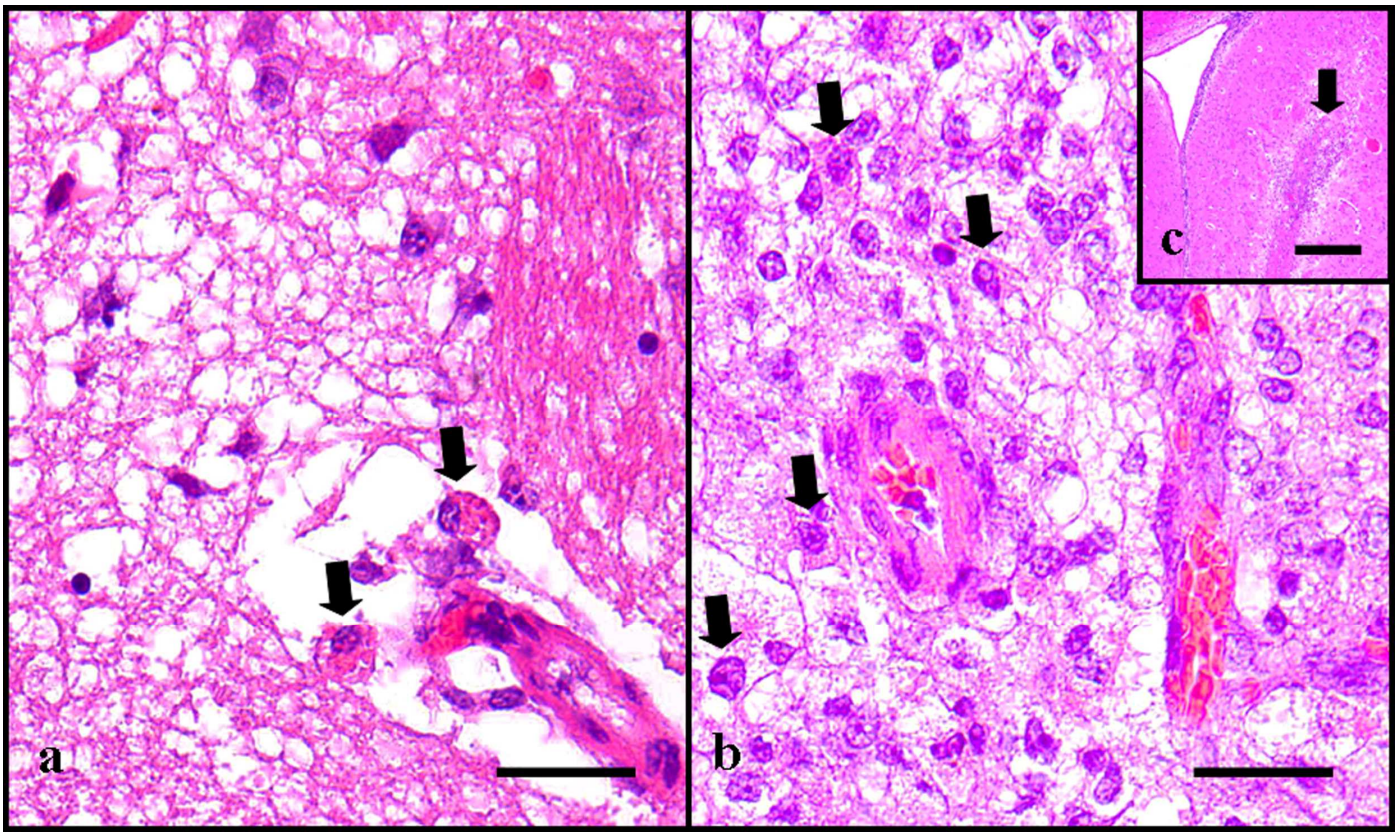

Figure 3-2. Malacic area in the ipsilateral striatum 24 h **(a)** and 5 d **(b)** after 6-OHDA intrastriatal injection. By 24 h, macrophages presented an increased cytoplasmic volume with a big nucleus, which, in most of the cells, was pushed aside to the periphery (black arrows in **a**). By 5 d, reactive cells dominated the lesion. Most of these cells exhibited paled cytoplasm swollen with ingested material (black arrows in **b**). Micrograph **c**: representative image of the ipsilateral striatum in control (5 d), in which the injection of vehicle solution produced non-specific damage at the injection site (black arrow) with no signs of malacia or important inflammation. H&E. Scale bars = 20 µm (a and b) and 200µm (c).

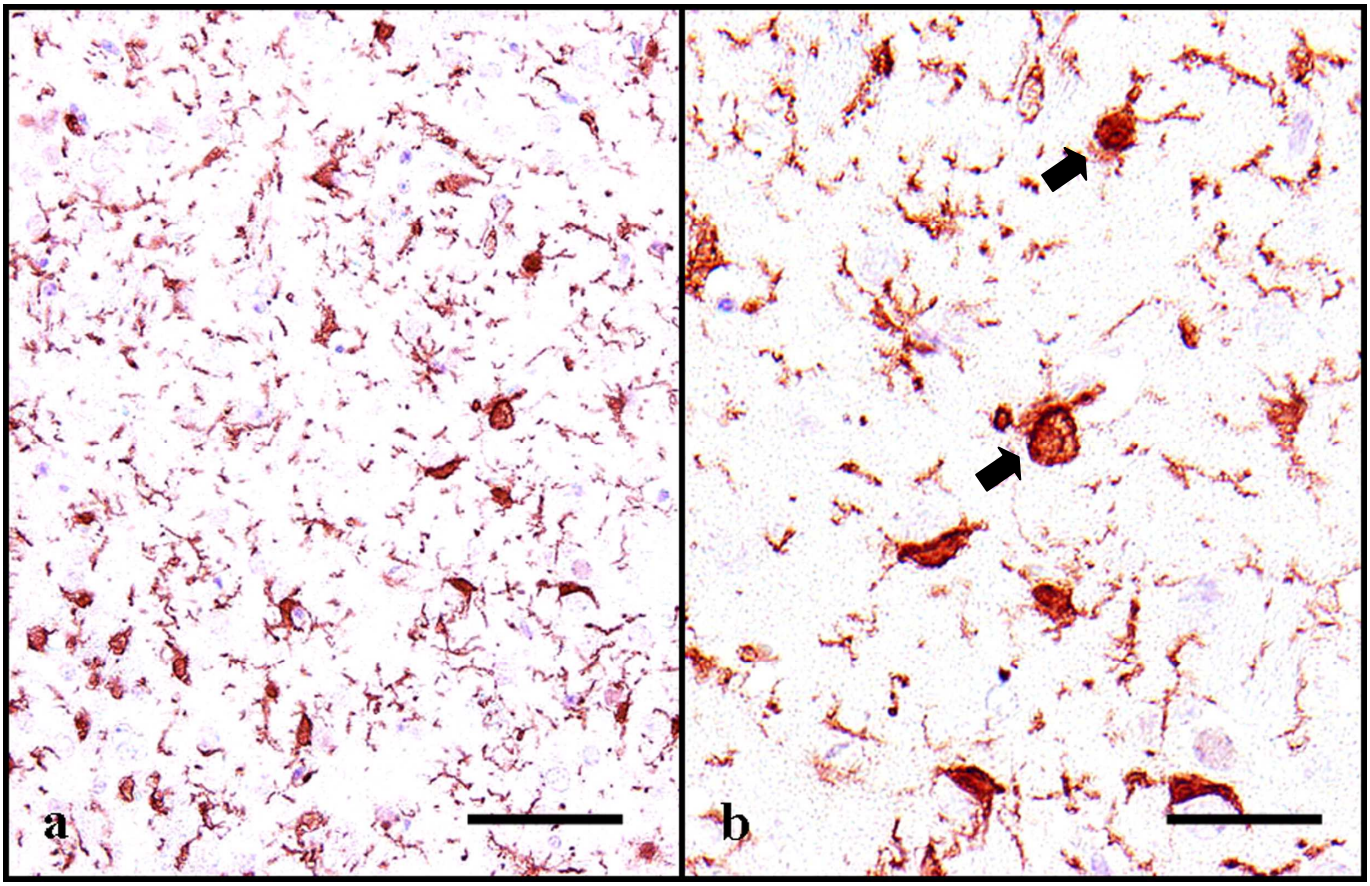

Figure 3-3. Representative micrographs of immunohistochemistry staining for Iba-1 in the ipsilateral (right) striatum 6 h post-injection. Most of these cells showed thick processes and a rounded appearance as the cytoplasmic volume was increased (black arrows in **b**). Micrograph **b** is a higher magnification of the micrograph **a**. Scale bars = 50 µm (a) and 20µm (b).

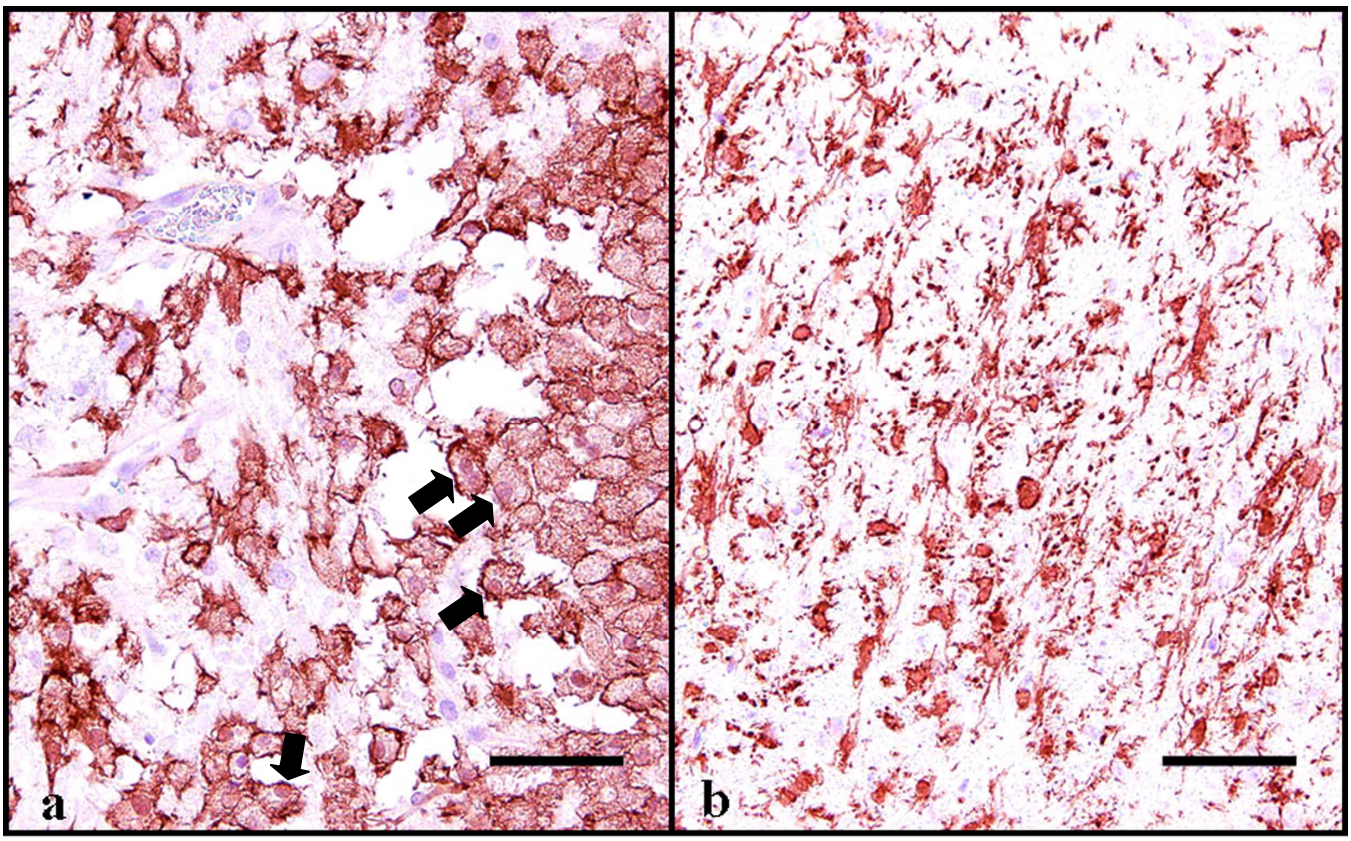

Figure 3-4. Representative micrographs of immunohistochemistry staining for Iba-1 in the ipsilateral (right) striatum **(a)** and SNpc **(b)** in the 6-OHDA-injured GH 5 d after the injection. Cells in the striatum showed pale cytoplasm and no definite processes. The cytoplasm of these cells became packed with ingested material, so that the nucleus was often pushed aside to the cell periphery (black arrows). Cells in the SNpc exhibited short and thick processes, as the Iba-1-positive cells observed in the striatum a few hours after 6-OHDA injection. Scale bars = 50 µm (a and b).

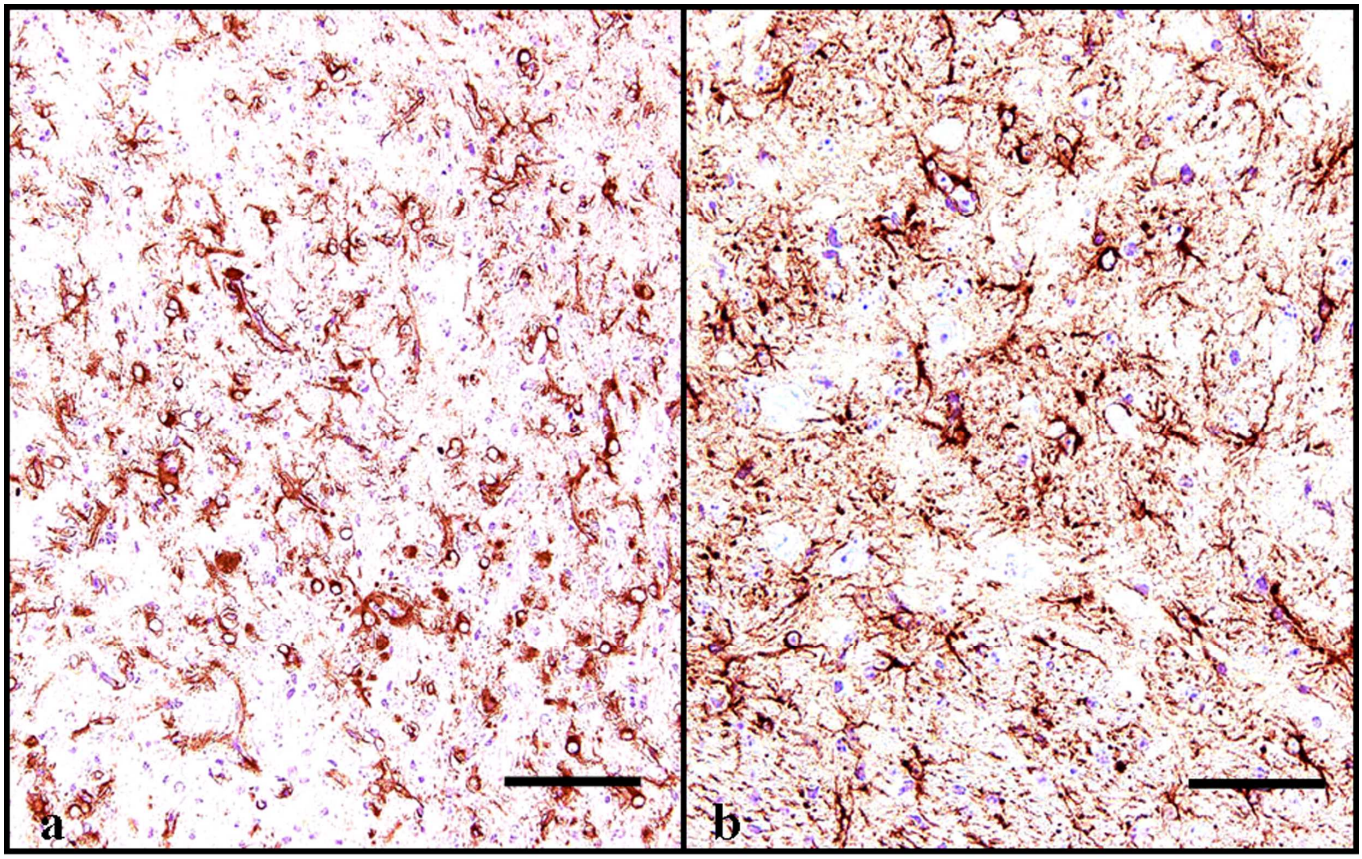

Figure 3-5. Representative micrographs of immunohistochemistry staining for GFAP in the ipsilateral (right) striatum **(a)** and SNpc **(b)** in the 6-OHDA-injured GH 5 d after the injection. GFAP immunostaining showed large cells with thin, long processes and pale nuclei. Scale bars = 100 µm (a) and 50µm (b).

Chapter 4

Neuroinflammation in the 6-OHDA-injured GH: roles of TNF-α and iNOS in this neurodegenerative model

Abstract

In chapters 2 and 3, I demonstrated that the intrastriatal injection of 6-OHDA in the GH induces degeneration of TH-immunopositive neurons of the SNpc accompanied by an active immune response in the nigrostriatal axis, which is characterized principally by a proliferation of Iba-1 positive microglial cells. In the present chapter, to investigate whether the attenuation of this inflammation influences the onset and progression of the dopamine cell degeneration, 6-OHDA-injected GH received a co-treatment of: i) MINO, ii) Pred or iii) MINO+Pred. Immunohistochemistry for TH, Iba-1 and GFAP was used to evaluate lesions in the nigrostriatal axis and the amount of activated microglia and astroglia, respectively. RT-PCR was used to measure the mRNA expression levels of cytokines, RNS and trophic neuroprotective factors. The results showed that the three anti-inflammatory treatments dramatically reduced activated microglia in the nigrostriatal axis. In addition, the TH-immunopositive areas in the ipsilateral striatum of either MINO- or Pred-treated animals were higher than that of control group. However, only in Pred group this TH recovery was statistically significant. mRNA measurements demonstrated lower expression levels of TNF-α, iNOS, BDNF and GDNF in Pred group

when compared with controls. Extending the observations made in Chapter 2, the results of the present chapter also demonstrate that TH-immunopositive fibers in the striatum have the ability to recover after 6-OHDA-induced toxicity of dopaminergic neurons and this recovery may occur due to a decrease in the microglial production of TNF-α and iNOS. In addition, this recovery may occurred by a mechanism independent of BDNF/GDNF actions.

Introduction

The typical pathological features observed in PD include the accumulation of alpha synuclein in Lewy body inclusions [91] and the degeneration of dopamine neurons in the SNpc [92]. Additionally, extensive microglia activation occurs in the brain parenchyma of patients with sporadic PD [52, 93], of humans exposed to the neurotoxin MPTP [94] and of animals treated with MPTP or 6-OHDA [95-98]. Microglia, the resident macrophages in the brain parenchyma, is considered to be the first line of defense in the central nervous system (CNS). When some pathological changes occur in the microenvironment of the CNS, glial cells (especially microglia and astrocytes) express the major histocompatibility complex (MHC) antigen in their membranes [5]. Subsequently, microglial cells swell, thicken their proximal processes and reduce the number of distal processes [99], becoming phagocytic and motile cells. Once activated, microglial cells release some trophic factors necessary for the development and sprouting of dopamine neurons such as BDNF and GDNF, and scavenge cellular debris and modified proteins (e.g. alpha synuclein) that normally are not present in the intercellular space [4].

On the other hand, activated microglia also release pro- (IL-1α, IL-1β, IL-6, INF-´Y, TNF-α) and anti-inflammatory (IL-4, IL-10, TGFβ1) cytokines, as well as ROS and RNS. The severity of the lesions depends on a delicate balance between the releases of pro- and anti-inflammatory substances, ROS and RNS.

In the present chapter, I examined whether the attenuation of neuroinflammation influences the onset and progression of the dopamine cell degeneration in the GH hemiparkinsonian 6-OHDA model.

Material and methods

Animals

Forty 10- to 12-week-old male GHs (*Mesocricetus auratus*) (SLC, Tokyo, Japan) weighing 90 to 120 g at purchased were used in this study. Animals were housed individually in a temperature-controlled (23 ± 2 °C) room with a constant level of humidity (55 ± 5%) under a 12/12 h light/dark cycle and free access to food and water. The procedures used in the present study were approved by the Committee of Animal Experiments, Graduate School of Agricultural and Life Science, the University of Tokyo. All the efforts were made in order to reduce the number of animals and their suffering.

Intrastriatal injection of 6-OHDA

Intrastriatal injection of 6-OHDA was performed as described in **Chapter 2**. For details, see Materials and methods; Intrastriatal injection of 6-OHDA; page 36.

Experimental design

Two anti-inflammatory drugs were used in this study: minocycline hydrochloride (MINO) was purchased from Sigma-Aldrich Japan K.K., Tokyo, Japan, while methylprednisolone (Pred) was purchased from Kyoritsu Seiyaku Corporation, Tokyo,

Japan. The drugs were diluted in a sterile 0.9% NaCl solution and injected intraperitoneally (ip) (MINO) or subcutaneously (sc) (Pred). Control animals were intrastriatally injected with 6-OHDA and received saline solution ip (controls for MINO group), sc (controls for Pred group) or ip + sc (controls for MINO+Pred group) instead of the anti-inflammatory treatment, following the same scheme as for the treated groups.

The outline of the treatments, together with the doses used in each of these treatments is summarized in **Fig 4-1**.

Tissue preparation

At day 5 after 6-OHDA intrastriatal injection (acute paradigm), animals were euthanized by a cervical dislocation after being deeply anesthetized with diethyl ether. The brain was exteriorized by removing the calvarium, removed and fixed in a 10% neutral-buffered formalin solution. After 48h fixation, 4-µm-thick paraffin sections, encompassing the complete striatum and SNpc, were prepared.

Immunohistochemistry

Paraffin sections were used for immunohistochemistry with the following primary antibodies: i) rabbit anti-Iba1 (1:500, Wako Pure Chemical Industries, Osaka, Japan) as

a microglia marker, ii) rabbit anti-TH (1:400, Millipore, Temecula, CA) as a dopaminergic neuron marker and iii) rabbit anti-GFAP (1:500; DAKO, Carpinteria, CA) as an astrocyte marker.

For antigen retrieval, deparaffinized sections were autoclaved at 121°C for 15 min. Endogenous peroxidase activity was blocked by incubating the sections with 3% hydrogen peroxide in methanol at room temperature for 5 min. For blocking nonspecific reaction, the sections were further treated with skimmed milk at 37°C for 40 min. The sections were then incubated at 37°C for 1 h with the primary antibodies. Thereafter, the sections were incubated with the Envision polymer reagent (DAKO Japan, Kyoto, Japan) at room temperature for 40 min and then visualized using 0.05% 3,3-diaminobenzidine (DAB) with 0.03% hydrogen peroxide in Tris–HCl buffer, before being counter-stained with methyl green (for TH) or hematoxylin (for Iba-1 and GFAP).

Measurements and statics (immunohistochemistry)

Serial brain coronal tissue specimens were obtained according to “A stereotaxic atlas of the golden hamster brain” [36]. At least 5 specimens in the SNpc (encompassing the entire rostrocaudal extent of the SNpc) and 8 specimens in the striatum per animal were

blindly applied for quantitative analyses.

Cells (SNpc) and positive areas (striatum) were quantified using Image J software (http://rsb.info.nih.gov/ij/). The procedures to quantify positive cells were performed as follows: once stained, tissue sections were viewed with an Olympus BX50 microscope (magnification x10) and one picture per specimen was taken using a Nikon DXM1200F digital camera. The images were then converted to grayscale binary image (8 bit) and a limit of threshold was adjusted in order to select only cells with a size > 600 pixel^2 and circularity between 0.1 and 1.0 (for TH) or a size > 500 pixel^2 and circularity between 0.1 and 1.0 (for Iba-1). After founding the optimal threshold, the cells were counted using the function “Analyze Particles”. However, due to the irregular shape and size of astroglial cells in the SNpc, cell counting for GFAP in this area was avoided. Instead, GFAP-positive area in the SNpc was measured as detailed below.

In the striatum, non-overlapping digital photomicrographs from both hemispheres (ipsilateral and contralateral striatum) were captured using a Nikon COOLSCAN IV ED (LS-40 ED) digital scanner with a magnification of x8. Eight sequential photomicrographs per animal, extending approximately from +2.5 mm to -0.5 mm with

respect to the bregma, were obtained. The images were then converted to grayscale binary image (8 bit) and the limit to threshold area function within Image J software was used to calculate a semi-quantitative index of the relative areas of each antibody. For statistical purposes, control group was given a relative value of 1 and the results in the treated group are expressed as relative values with respect to that of the control group. Two-way ANOVA test was performed to assess potential differences between control and treated groups. Differences were considered statistically significant when $p < 0.05$. The normal distribution for each group of animals was checked using a normal probability plot and the homogeneity of variance was checked using f-test for two samples.

RNA extraction and RT-PCR

At necropsy, the striatum and SNpc were sampled and immediately homogenized in the ISOGEN fluid (Nippongene, Tokyo, Japan) using the Tissue-ruptor (Qiagen, Valencia, CA, USA). RNA extraction was performed through the treatment of sample tissues with chloroform, precipitation in isopropanol and washing with 75% ethanol. To know the concentration of the resulting RNA, samples were measured with a

spectrophotometer using an absorbance of 260 nm. Then, the RNA was eluted in RNase-free water and stored at -80°C until use.

Reverse transcription (RT) was performed using the PrimeScript RT reagent kit (Takara Biotechnology, Dalian, China), according to the manufacturer's instructions. Briefly, 1 μg/μl of RNA was mixed with 2.5 μM Oligo dT primer, dNTP mixture and RNase free water, to make a total volume of 20 μl. The mixture was kept at 70°C for 10 min. Then, 5x PrimerScript buffer, RNase inhibitor, RNase free water and PrimeScript RTase enzyme were added to make a final volume of 40 μl. The mixture was kept at 42°C for 50 min and the reaction stopped at 70°C. Finally, to inactivate the enzyme activity, the mixture was kept at 99°C for 5 min.

For RT-PCR, the ExTaq Enzyme Hot Start PCR kit (Takara Biotechnology) was used according to the manufacturer's instructions. The primers used for RNA amplification are shown in **Table 4-1**. PCR of the cDNA was performed as follows: dissociation at 94°C for 30 s, annealing at 55°C for 30 s with an extension at 72°C for 30 s. The cycles of the reaction were 34 (for BDNF), 36 (for TNF-α), 38 (for IL-1β, IL-6, INF-α, INF-΄Y, iNOS, GDNF and TGF-β1) or 40 (for IL-10), with an extension at 72°C for 10 min.

Measurements and statics (RT-PCR)

2% agarose gel electrophoresis was performed and the bands of the products were stained with GR Red Loading Buffer (BIO CRAFT Co., Tokyo, Japan) and observed using the Molecular Imager® ChemiDoc™ XRS+ system (BIO RAD, Tokyo, Japan). The ratio of the intensity of a specific band to that of a house-keeping gene (β-actin) was calculated using the Image Lab™ Beta 2.0 software (BIO RAD laboratories, Tokyo, Japan). Relative mRNA expression levels are shown as the mean ± standard deviation (SD). Two-way ANOVA test was used to assess the differences between data groups.

Results

MINO, Pred or MINO+Pred treatments induce a marked reduction in the Iba-1-immunoreactivity (Fig. 4-2)

In 6-OHDA alone injected animals (control group), there was a 250% increase of the Iba-1-positive area in the ipsilateral (right) striatum when compared with the contralateral (left) striatum. When GH received 6-OHDA and a concomitant treatment with MINO, Pred or MINO+Pred, the ipsilateral Iba-1-positive areas showed a 40%, 34% or 62% decrease, respectively, when compared with the ipsilateral striatum in control group **(Fig. 4-2.k, white bars)**. These results show that the three treatments were able to significantly decrease the Iba-1-positive areas in the ipsilateral striatum of 6-OHDA-injected GH. On the other hand, the contralateral hemisphere showed no significant changes between control and treated groups **(Fig. 4-2.k, black bars).**

In the ipsilateral SNpc, the three treatments reduced the number of Iba-1-positive cells when compared with controls, although MINO and Pred individual treatments achieved a statistically significant reduction **(Fig. 4-2.l)**.

Pred treatment induces a recovery in the TH striatal immunoreactivity (Fig. 4-3)

In the ipsilateral striatum of the control group, I found a markedly reduction of the TH-positive area by up to 70% when compared with the contralateral striatum. When GH received 6-OHDA and a concomitant treatment with MINO, Pred or MINO+Pred, the ipsilateral TH-positive areas were approximately a 36%, 100% or 30% higher, respectively, when compared with the ipsilateral striatum in control group **(Fig. 4-3.a, white bars)**, suggesting the possibility that TH-positive fibers recovered after injury. Statistically, only Pred-treatment was able to significantly rescue the decrease of TH-positive dopamine fibers in the ipsilateral striatum. On the other hand, the contralateral hemisphere showed no significant changes in the TH-positive areas between control and treated groups **(Fig. 4-3.a, black bars)**. Representative cases from each of the treated groups and the lesioned control are illustrated in **Fig. 4-3.c**.

TH-immunopositive neurons in the SNpc (Fig. 4-3)

In the ipsilateral SNpc of the control group, I found a markedly reduction of TH-positive cells by up to 13.8% when compared with the contralateral striatum ($p < 0.01$) On the other hand, the number of TH-positive cells in the ipsilateral SNpc of

MINO-, Pred- and MINO+Pred-treated groups were reduced by up to approximately 7.6%, 4.9% and 12.1%, respectively, when compared with the contralateral side **(Fig. 4-3.b)**. Thus, the lack of statistically significant differences in the number of TH-immunopositive neurons between the ipsilateral and contrlateral SNpc in the three treated groups may be the result of a protective effect of the drugs in the SNpc. Representative cases from the ipsilateral and contralateral SNpc of each of the treated groups and the lesioned control are illustrated in **Fig. 4-3.c**.

MINO, Pred or MINO+Pred treatments do not affect the GFAP-immunoreactivity (Fig. 4-4)

Control group animals showed a 165% increase of the GFAP-positive area in the ipsilateral striatum when compared with the contralateral striatum. When GH received 6-OHDA and a concomitant treatment with MINO, Pred or MINO+Pred, the ipsilateral GFAP-positive areas showed a 6.4% increase, 17% or 25.4% decrease, respectively, when compared with the ipsilateral striatum in control group **(Fig. 4-4.k, white bars)**. Despite these differences, none of the treatments significantly affected the GFAP-positive areas in the ipsilateral striatum of 6-OHDA-injected GH. On the other

hand, the contralateral hemisphere showed no significant changes between control and treated groups **(Fig. 4-4.k, black bars).**

In the ipsilateral SNpc, there were no significant differences in the GFAP-positive areas between control and treated groups **(Fig. 4-4.l)**.

Gene expression

To further explore the reasons for the higher TH-immunoreactivity in the ipsilateral striatum observed in the Pred group, and to explore the reasons for the weak neuroprotection observed in the MINO and MINO+Pred groups after a single intrastriatal administration of 6-OHDA, mRNA levels of cytokines (IL-1β, IL-4, IL-10, INF-α, INF-΄Y, TNF-α and TGF-β1), RNS (iNOS) and neurotrophic protective factors (BDNF and GDNF), were measured. The mRNA expression levels of TNF-α and iNOS in the ipsilateral (right) striatum and SNpc of Pred-treated animals were significantly reduced when compared with controls **(Fig. 4-5.a** and **b**, respectively**)**. In addition, Pred-treated animals expressed significantly lower mRNA levels of BDNF and GDNF in the ipsilateral striatum and SNpc **(Fig. 4-5.c** and **d,** respectively**)**. On the other hand, no significant differences were found in the mRNA expression levels of

anti-inflammatory cytokines (TGF-β1, IL-4 and IL-10) **(Fig. 4-6)** or pro-inflammatory cytokines (IL-1βI, INF-α and INF-´Y) **(Fig. 4-7)** between treated groups and controls.

Discussion

The present findings demonstrate that the TH-immunopositive fibers in the striatum have the ability to recover after 6-OHDA-induced toxicity of dopaminergic neurons, and this recovery may be due to a decrease in the microglial production of TNF-α and iNOS. The possible events involved in dopaminergic terminal degeneration and recovery are summarized in **Fig. 4-8**.

In the present chapter, prednisolone at a dose of 2 mg/kg or minocycline at a dose of 45 mg/kg were used with the aim of inhibiting part of the activated microglia in the nigrostriatal axis in order to evaluate whether the attenuation of neuroinflammation influences the onset and progression of the lesions induced by 6-OHDA.

Prednisolone has been shown to have neuroprotective effects, possibly by inhibiting oxygen free radical-induced lipid peroxidation [100]. *In vitro* studies have showed that prednisolone treatment induces important reductions in the levels of some cytokines [101-102]. Meanwhile, minocycline, a second generation tetracycline, has been described as an effective neuroprotective agent in experimental models of brain ischemia [103-104] and traumatic brain injury [105]. In addition, it has been previously

used to confer neuroprotection in the MPTP and 6-OHDA models of PD [106-107]. However, recent studies have shown that minocycline, although inhibiting the activated microglia, exacerbates MPTP-induced damage to nigrostriatal neurons [108-109]. These contradictory data suggest that minocycline could display either a protective or an exacerbating role in a neurotoxic model of PD according to the conditions in which it is administered.

In the present chapter, both individual treatments significantly attenuated the number of microglial cells in the nigrostriatal axis and the TH-positive areas in the ipsilateral striatum of either prednisolone- or minocycline-treated animals were higher than that of control group. However, only in the prednisolone group this TH recovery was statistically significant. The histologic recovery of TH-immunopositive fibers exerted by prednisolone strongly suggests that some factors released by activated microglia have a powerful trophic effect on dopaminergic neurons. The fact that prednisolone reduced the levels of some cytokines in the SNpc coincided with an important protection of the ipsilateral TH-positive neurons (only 4.9% reduction when compared with the contralateral, noninjured SNpc, as shown in the Results section), and suggest a

relationship between the protection of SNpc neurons and the possibility of a regeneration in the striatum. This idea is in full agreement with previous reports in which the capacity of regenerative sprouting after nigrostriatal injury occurred when TH-positive cell bodies in SNpc were not affected during the recovery phase [76]. This fact may also explain why in minocycline-treated animals, in which TH-positive neurons in the ipsilateral SNpc decreased by a 7.6%, the TH-positive fibers in the ipsilateral striatum do no statistically recovered at day 5 after the injury. The study of cytokines in striatum and SNpc at day 5 after 6-OHDA injection leads to the question of the molecules involved in the nigrostriatal degeneration, and two obvious candidates are TNF-α and iNOS, because both of them are statistically reduced in the ipsilateral striatum and SNpc of the prednisolone group.

Deleterious effects of TNF-α in neurodegeneration have been documented [87]. TNF-α can stimulate activated microglia to release chronically elevated levels of pro-inflammatory cytokines, which induce a vicious circle with self-perpetuation of the neuroinflammation and the concomitant damage of dopamine neurons in the SNpc [110]. My present observations are consistent with previous reports where, using the MPTP or

methamphetamine (METH) model of PD, minocycline was proved to attenuate microglial activation but failed to protect dopaminergic cells, probably due to its inability to reduce TNF-α levels in the striatum [111]. On the other hand, iNOS, a nitric oxide synthase (NOS) isoform, may also initiate and amplify the oxidative damage by inducing reactions with the anion superoxide, which is converted to peroxynitrite [112]. Normally absent in the brain, iNOS is expressed by astrocytes and microglial cells under pathological conditions [113-114]. Considering that the use of specific iNOS-inhibitors induced a neuroprotective response [115], and that the treatment with glucocorticoids has been described to inhibit an NOS isoform [114], the most likely possibility is that prednisolone, apart from reducing TNF-α levels, also reduces the iNOS expression levels, which may contribute to protect TH-positive cell bodies in the SNpc during the recovery phase.

An interesting observation in my study is the close correlation between TNF-α and trophic neuroprotective factor levels. *In vitro* studies have demonstrated that TNF-α contributes to the up-regulation of BDNF and GDNF [116-117], which are possible therapeutic molecules to treat PD [118-120]. In addition, GDNF has been described as a

neuroprotectant factor in the 6-OHDA model of PD [121-122]. *In vivo*, neurons and glial cells can release BDNF and GDNF [123]. In the present study, lower TNF-α expression levels in the prednisolone group correlated with lower mRNA expression levels of BDNF and GDNF in the ipsilateral striatum. However, the recovery of TH-immunopositive fibers in the striatum seems not to be affected by these lower levels. Thus, these results suggest that the TH-regeneration in the ipsilateral, injured striatum, at least in the acute recovery phase, may occur by a mechanism/s independent of BDNF/GDNF.

In this study, there were no statistical differences in the mRNA expression levels of the measured cytokines between the ipsilateral and the contralateral, noninjured striatum. These results may suggest the possibility that, after a hyperacute phase post injury, the levels of some cytokines such as TNF-α and iNOS tend to decrease. This suggestion may be supported by the observation of Barcia et al. [124], who have reported that mice, unlike non-human primates, merely show a transitory increase in pro-inflammatory cytokines from 24 h to 72 h after MPTP administration.

A particularly relevant observation in my study is the lack of TH-positive fibers' recovery in the animals treated with a combination of minocycline and prednisolone. Combination therapy of two drugs could be advantageous if both drugs have: i) different mechanisms of action; ii) good safety profiles; and iii) no additional toxicities when implemented together [125]. Apparently, minocycline and prednisolone fit these requirements and some studies have described beneficial effects of the combination [126-127]. In the present study, however, the combination therapy did not improve the striatal TH-immunoreactivity whereas prednisolone did improve it when administered alone. The results may be explained by the difference in the dosing regimen employed. In studies in which MINO+Pred treatment achieved beneficial effects, both drugs were administered at suboptimal doses [126-127], while in my study minocycline was administered in a high-dose regimen. Thus, it may be possible that, at lower doses, minocycline does not influence the action of prednisolone achieving a synergic effect, while at higher doses minocycline may change the pharmacokinetic and/or pharmacodynamic actions of prednisolone by, for instance, displacing it from its bindings and/or modifying its binding pattern to tissue or to plasma components. Thus,

in the absence of prednisolone effects on activated microglial cells, the results observed in the MINO+Pred group reflect those observed in minocycline group. In addition, I suggest that the slightly more potent inhibition of microglial cells by the combination therapy (as evidenced by Iba-1 immunostaining) is not the result of a synergistic effect of both drugs but the effect of a high dose regimen of minocycline.

In summary, taken together, the findings generated in the present chapter demonstrate that: i) the inhibition of TNF-α and iNOS production after a neurotoxic insult helps to prevent dopaminergic cell degeneration in the SNpc; ii) these surviving neurons are the basis for the regenerative sprouting of TH-positive fibers in the striatum during the recovery phase; and iii) during this acute phase, the TH-immunopositive fibers' recovery may occurred by a mechanism independent of BDNF/GDNF actions. As in the present chapter TNF-α and iNOS were proved to be involved in the lesions of the nigrostriatal axis after a single intrastriatal injection of 6-OHDA, it seems plausible that they, among others, may also be involved in the vulnerability of dopaminergic cells in the sporadic PD.

Table 4.1. Sequences of the primers used in the present chapter

Gene		Primer sequence
ß-actin	Forward	GTTTGAGACCTTCAACACCCA
	Reverse	GATGTCAACGTCACACTTCA
BDNF	Forward	GCGGCAGATAAAAAGACTGC
	Reverse	CTTATGAAACGCCAGCCAAT
GDNF	Forward	TAATGTCCAACTGGGGGTCT
	Reverse	CGCTTCGAGAAGCCTCTTAC
IL-1ß	Forward	GGCTGATGCTCCCATTCG
	Reverse	CACGAGGCATTTCTGTTGTTCA
IL-4	Forward	CCACGGAGAAAGACCTCATCTG
	Reverse	GGGTCACCTCATGTTGGAAATAAA
IL-6	Forward	CTCCGCAAGAGACTTCCATC
	Reverse	ACCAAACCTCCGACTTGTTG
IL-10	Forward	GTTGCCAAACCTTATCAGAAATGA
	Reverse	TTCTGGCCCGTGGTTCTCT
INF-a	Forward	TCGTTGCTGCTCCCGTAGTC
	Reverse	ATGGATCCCGCTGCAATTC
INF-?	Forward	GGCCATCCAGAGGAGCATAG
	Reverse	TTTCTCCATGCTGCTGTTGAA
iNOS	Forward	TGCCTTGCATCCTCATTGG
	Reverse	GTCGCTGTTGCCAGAAACTG
TGF-ß1	Forward	TGTGTGCGGCAGCTGTACA
	Reverse	TGGGCTCGTGAATCCACTTC
TNF-a	Forward	GACGGGCTGTACCTGGTTTA
	Reverse	AGACCCCTCCCAGGTAGATG

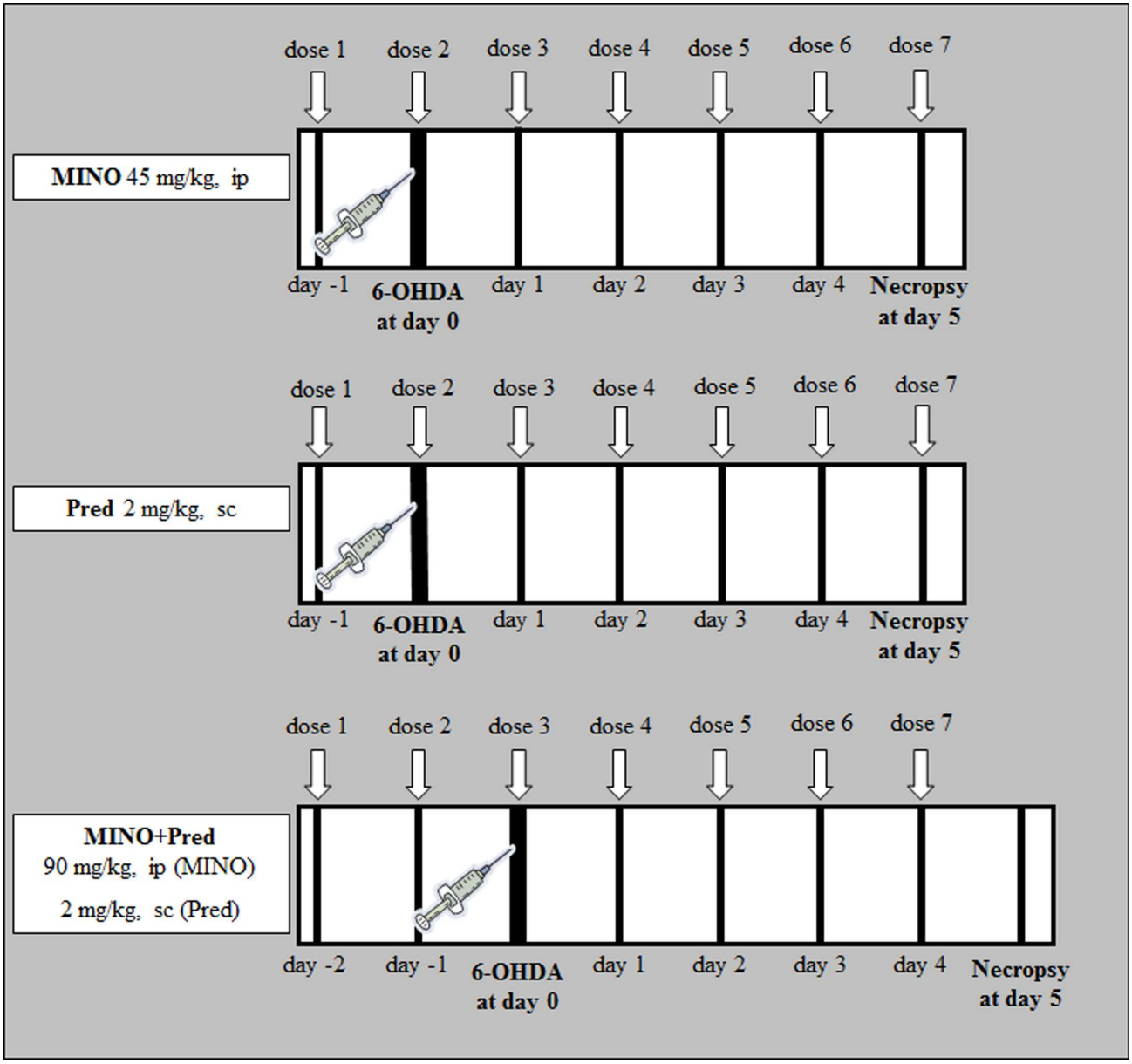

Figure 4-1. Schematic illustration of experimental designs.

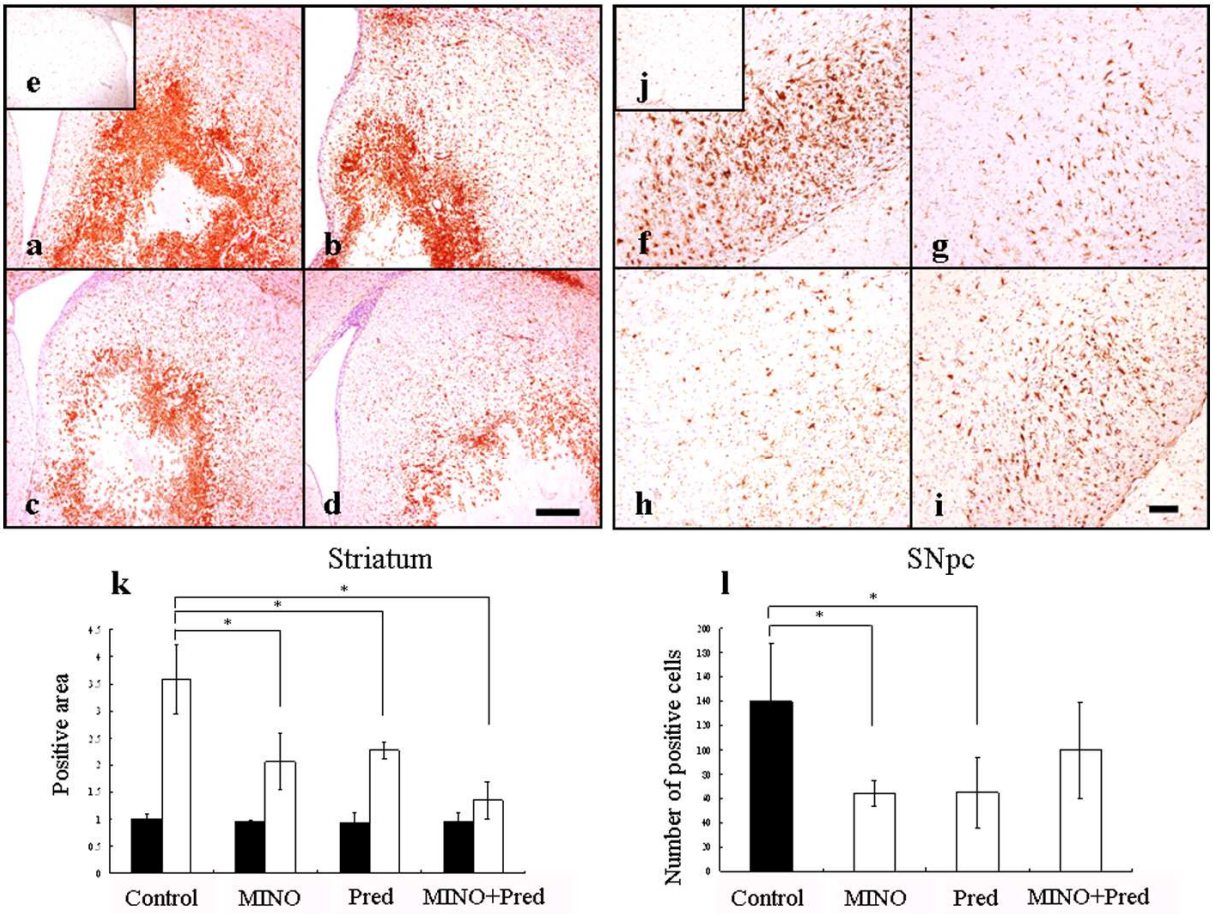

Figure 4-2. Results of Iba-1-immunostaining in the striatum **(a~e)** and SNpc **(f~j)** after a single 6-OHDA injection in control **(a and f)**, MINO- **(b and g)**, Pred- **(c and h)** and MINO+Pred- **(d and i)** treated groups. Figures **e** (contralateral striatum) and **j** (contralateral SNpc) show the lack of Iba-1-unspecific binding. Bars = 200 µm (a~d) and 100 µm (f~i). Graphs **k** and **l** show the quantification of Iba-1-positives areas and Iba-1-positive cells, respectively. ■ = Contralateral striatum and □ = Ipsilateral striatum in **k**. Values are expressed as the mean ±SD. $^{*}p < 0.05$; significantly different from the control group (n = 9 control, 3 MINO, 3 Pred and 3 MINO+Pred).

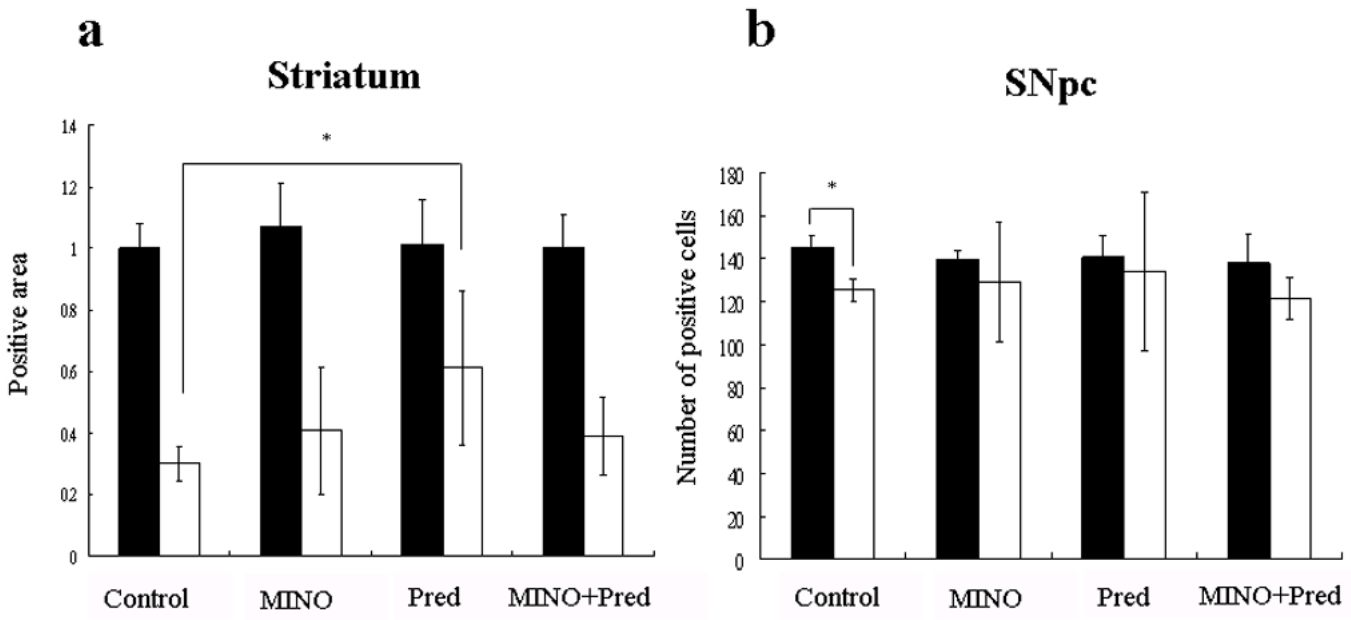

Figure 4-3. Results of TH-immunostaining after an intrastriatal injection of 6-OHDA. Graphs **a** and **b** show the quantification of the TH-positives areas and TH-positive cells, respectively. ■ = Contralateral striatum (a) or contralateral SNpc (b) and □ = Ipsilateral striatum (a) or ipsilateral SNpc (b). Values are expressed as the mean ± SD. $^{*}p < 0.05$; significantly different from the control group (a) or significantly different from the contralateral side (b) (n = 9 control, 3 MINO, 3 Pred and 3 MINO+Pred). **c)** Photomicrographs of nigrostriatal TH-immunoreactivity. Coronal sections of the striatum represent an area approximately between +0.5 mm～+0.1 mm with respect to the bregma. The cell counts in the mesencephalon were done at equally spaced levels and included only cells in the SNpc (for more details, see Materials and methods section in this chapter; page 75). Bar (pictures in SNpc) = 200 µm.

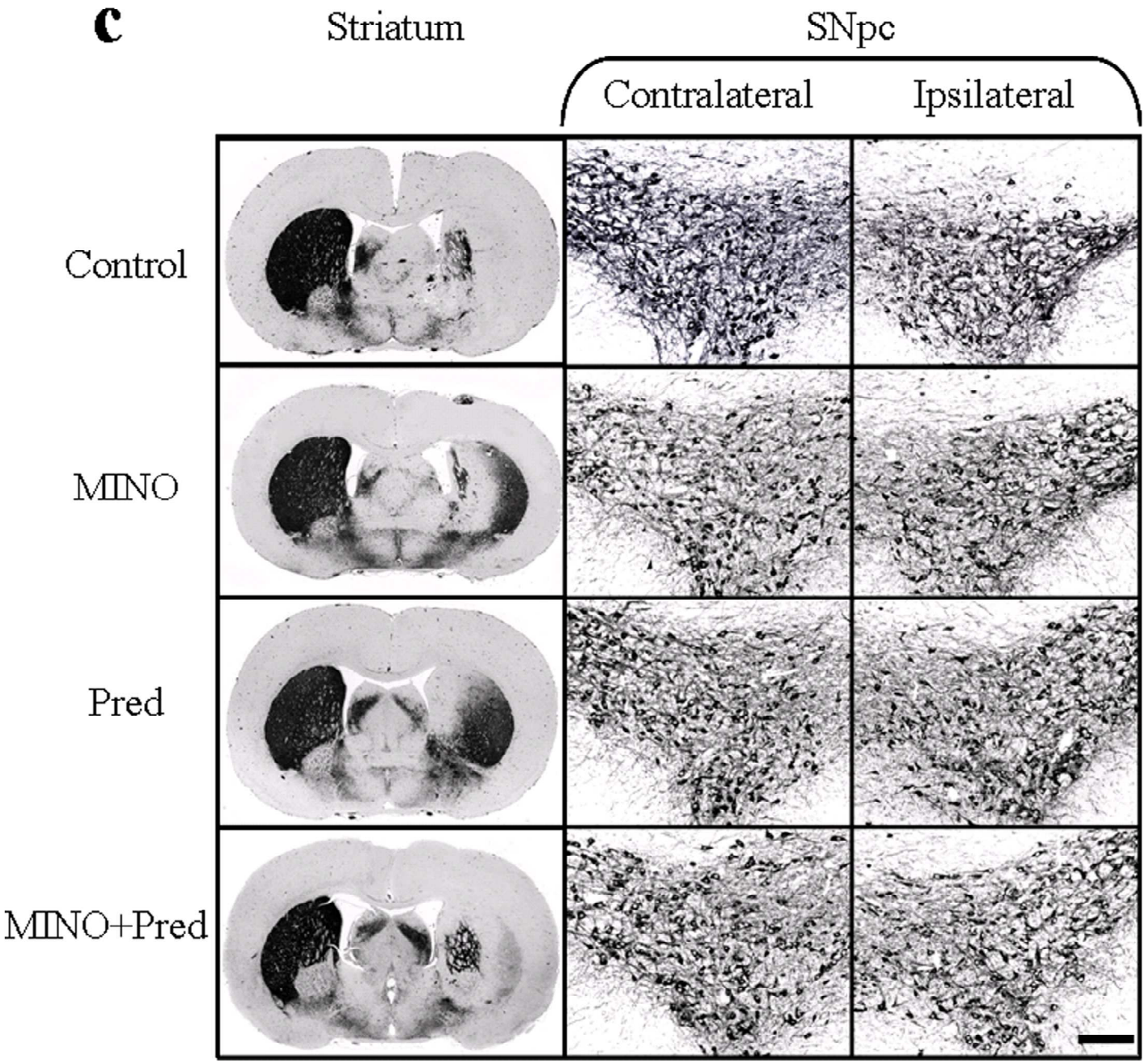

Figure 4-3-Continued

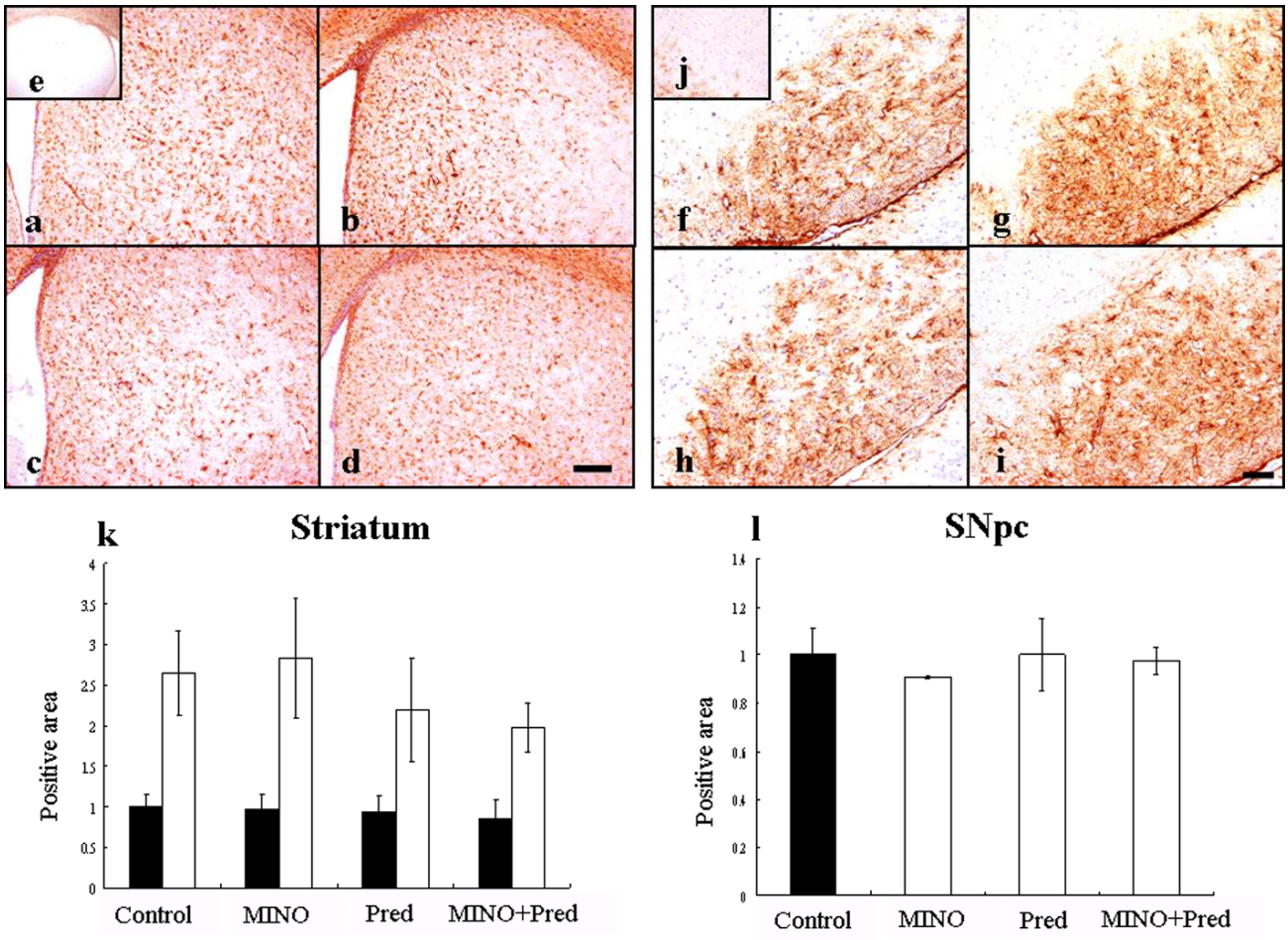

Figure 4-4. Results of GFAP-immunostaining in the striatum **(a~e)** and SNpc **(f~j)** after a single 6-OHDA injection in control **(a and f)**, MINO- **(b and g)**, Pred- **(c and h)** and MINO+Pred- **(d and i)** treated groups. Figures **e** (contralateral striatum) and **j** (contralateral SNpc) show the lack of GFAP-unspecific binding. Bars = 200 µm (a~d) and 100 µm (f~i). Graphs **k** and **l** show the quantification of GFAP-positives areas in the striatum and SNpc, respectively. ■ = Contralateral striatum and □ = Ipsilateral striatum in **k** (n = 9 control, 3 MINO, 3 Pred and 3 MINO+Pred).

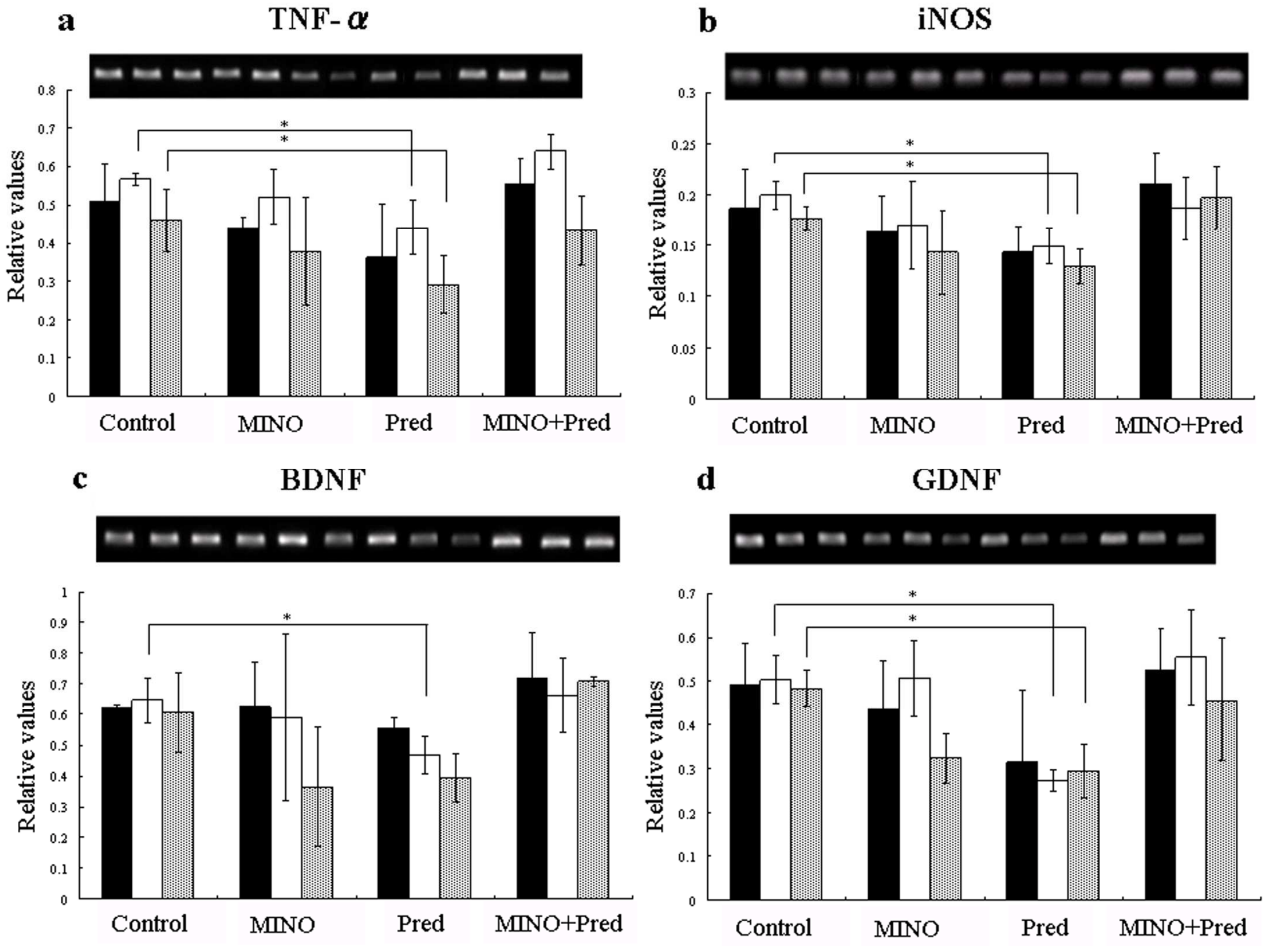

Figure 4-5. Relative mRNA expression levels of TNF-α **(a)**, iNOS **(b)**, BDNF **(c)** and GDNF **(d)** in GH intrastriatally injected with 20 μg of 6-OHDA. ■ = contralateral striatum; □ = ipsilateral striatum; and ▒ = SNpc. Panels, upper graphs: representative RT-PCR bands for control contralateral striatum; control ipsilateral striatum; control SNpc; MINO contralateral striatum; MINO ipsilateral striatum; MINO SNpc; Pred contralateral striatum; Pred ipsilateral striatum; MINO+Pred contralateral striatum; MINO+Pred ipsilateral striatum; and MINO+Pred SNpc, respectively. Values are expressed as the mean ±SD. $^{*}p < 0.05$; significantly different from the control group.

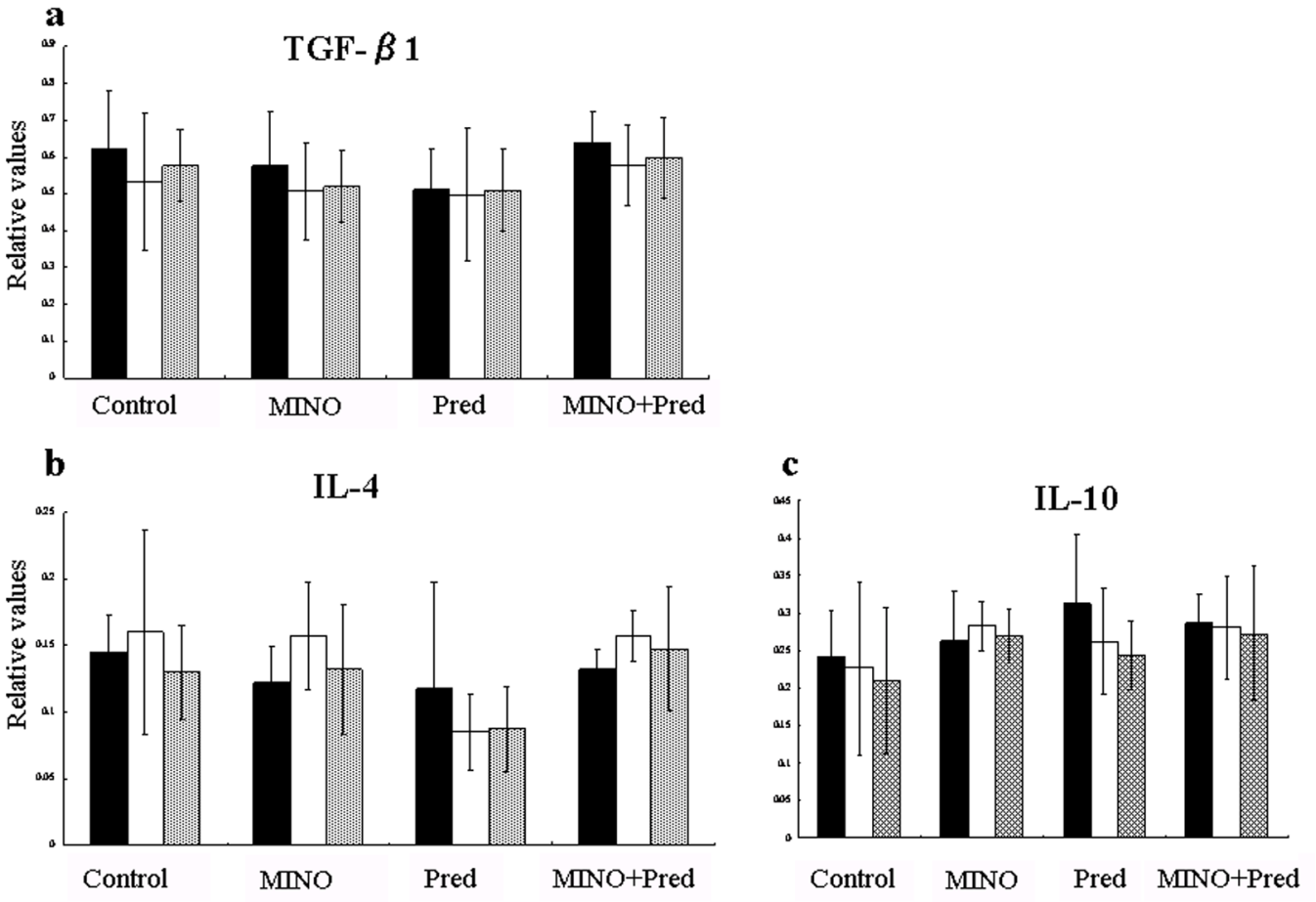

Figure 4-6. Relative mRNA expression levels of the anti-inflammatory cytokines TGF-β1 **(a)**, IL-4 **(b)** and IL-10 **(c)** in GH intrastriatally injected with 20 μg of 6-OHDA.

■ = contralateral striatum; □ = ipsilateral striatum; and ▒ = SNpc.

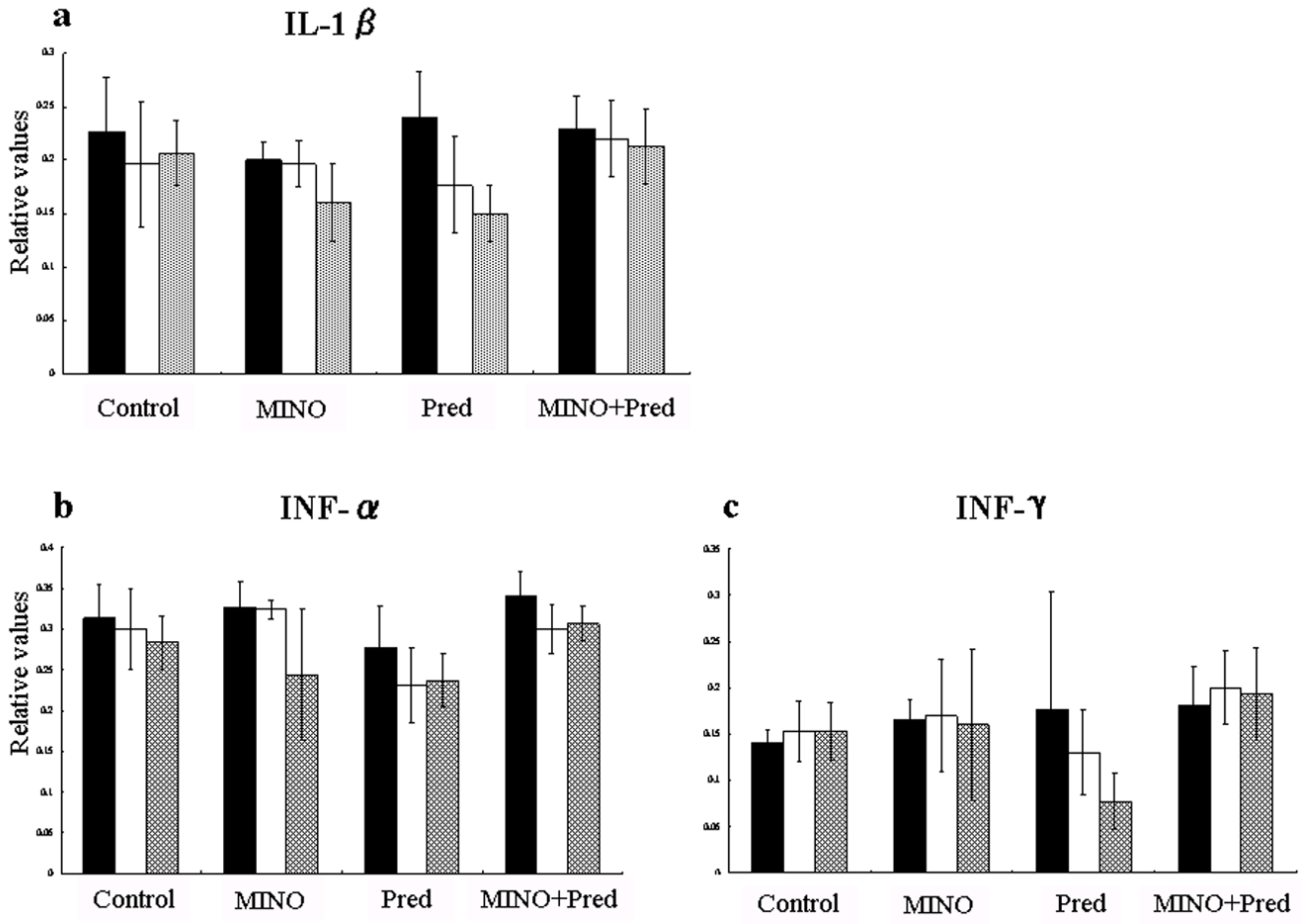

Figure 4-7. Relative mRNA expression levels of the pro-inflammatory cytokines IL-1β **(a)**, INF-α **(b)** and INF-´Y **(c)** in GH intrastriatally injected with 20 µg of 6-OHDA. ■ = contralateral striatum; □ = ipsilateral striatum; and ▒ = SNpc.

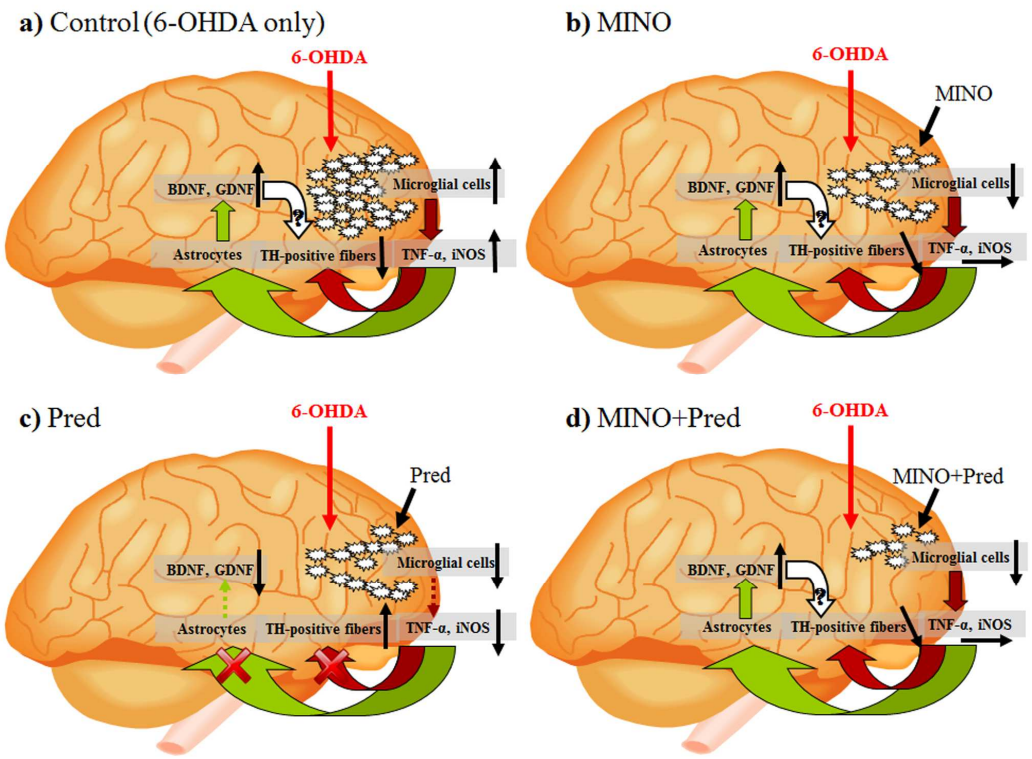

Figure 4-8. Possible mechanisms that lead to the striatal degeneration and recovery in a 6-OHDA GH model of PD. **a)** A single intrastriatal administration of 6-OHDA induces microglial activation in the ipsilateral side to the injection. Activated microglial cells release iNOS and TNF-α, which may stimulate astroglial cells to produce neurotrophic protective factors such as BDNF and GDNF. However, the elevated levels of TNF-α induce a vicious circle with self-perpetuation of the inflammation. **b and d)** Despite a markedly decrease in activated microglial cells, MINO- and MINO-Pred-treatments are not able to significantly reduced the levels of TNF-α and iNOS. **c)** Pred not only leads to a decrease in activated microglial cells but also to a significant decrease in TNF-α and iNOS expression levels with a concomitantly significant TH-immunopositive fibers' recovery.

Conclusions

Most of the toxin-induced parkinsonism studies have been conducted in the mouse and rat and very few of them, if not almost none, in the GH. Thus, in this thesis, I sought to extend the existing literature by examining the effects of two well-known neurotoxins, MPTP and 6-OHDA, upon the nigrostriatal axis of the GH that, as mentioned above, has hardly been used for neuropathological studies.

Chapter 1 dealt with the following questions: i) are the low levels of cerebral MAO-B in the GH the only responsible for the MPTP resistance? and ii) is it possible that the location of the enzyme, despite its low levels, also influence in this resistance? To address these questions, I immunohistochemically examined the expression of MAO-B in the brain. The results showed that MAO-B is predominantly expressed in the endothelial cells but not in the astrocytes. Then, to eliminate the need of MAO-B in the process, I directly injected the active and toxic compound MPP^+ into the cerebral ventricle. However, no alterations occurred in the nigrostriatal axis after this administration. Hence, taken together, the results of Chapter 1 suggest that:

1. BBB endothelial cells in the GH are the first barrier against systemically injected MPTP. When systemically administered, MPTP is converted to MPP^+ by

MAO-B present in the brain vessel endothelium. Since MPP^+ is a polar compound, it cannot cross the BBB.

2. GH is also resistant to MPTP regardless of the low levels or localization of cerebral MAO-B. The mechanisms underlying central resistance to MPP^+ need to be addressed in further investigations.

6-OHDA does not require MAO-B to exert its toxic effects and only when centrally administered induces neurotoxicity. These characteristics make 6-OHDA an ideal candidate to challenge the resistance of the GH to neurotoxins. For this reason, in **Chapter 2**, I intrastriatally injected 6-OHDA and subsequently presented an immunohistochemical study of the nigrostriatal axis of the challenged GH. The results showed that, unlike what happen with MPTP, the GH is sensitive to the effects of 6-OHDA-induced neurotoxicity, as evidenced by the decreases of TH- and DAT-immunostaining in treated animals in both striatum and SNpc.

Since 6-OHDA demonstrated to induce degeneration of TH- and DAT-positive cells within the ipsilateral nigrostriatal axis of the GH, **Chapter 3** was designed to determine whether cell death in the SNpc occurs through apoptosis and to characterize the

histopathology of the lesions that accompany the neurodegeneration induced by a single intrastriatal injection of 6-OHDA. As no apoptosis was detected in the SNpc, it was concluded that 6-OHDA may trigger an alternate form of programmed cell death in the nigrostriatal axis. In addition, as demonstrated by hematoxylin/eosin stain and immunohistochemistry for specific glia components, 6-OHDA triggers rapid and lasting microglial activation, characterized principally by proliferation of Iba-1 positive macrophages. On the basis of these results, **Chapter 4** was designed to assess whether the attenuation of this neuroinflammation influences the onset and progression of the dopamine cell degeneration induced by 6-OHDA. To achieve this goal, I intrastriatally injected 6-OHDA in GHs (as done in chapters 2 and 3) and co-treated these animals with one of the tree anti-inflammatory treatments: i) MINO, ii) Pred or iii) MINO+Pred. The results showed that Pred lead to a statistically significant TH-immunopositive fibers' recovery in the ipsilateral, 6-OHDA-injured striatum. Hence, taken together, the results of Chapters 2, 3 and 4 suggest that:

1. In the GH, a single intrastriatal injection of 6-OHDA induces neurotoxic effects upon dopaminergic neurons accompanied by an active microglial/macrophage

reaction.

2. TH-immunopositive fibers in the striatum have the potential ability to recover after 6-OHDA-induced toxicity of dopaminergic neurons.
3. The TH-immunopositive fibers' recovery observed in the GH co-treated with Pred strongly suggests that some factors released by activated microglia and inhibited by Pred (such as TNF-α and iNOS) have a powerful trophic effect on dopaminergic neurons.

Perspectives

On the one hand, one might think that, due to its resistance to MPTP-induced neurotoxicity, the GH is not an accurate model to study PD. However, a neurotoxin-based model of PD can be useful even without exerting lesions in the nigrostriatal axis. Deciphering the mechanisms (enzymatic conversion, faster clearance, reuptake, storage in vesicles, etc.) that confer resistance to a particular neurotoxin can have a significant impact on human health, for instance in the design of potential neuroprotective strategies.

One the other hand, despite its sensitivity to 6-OHDA, one might ask about the advantages of modeling PD in the GH and not in the rat, which is the animal *par excellence* to study the effects of this toxin. However, as PD can be modeled at different levels, it could result more convenient to think about how to complement these models. For instance, at the behavioral level, the 6-OHDA rat model of PD is (and probably will be) the most accurate to recapitulate the symptomatic stages of human PD in studies of functional recovery aimed at developing neuroprotective strategies; at the histological level, the 6-OHDA GH model of PD could result an interesting option in studies aimed at confirming the contribution of the inflammation in neurodegeneration.

In other words, as a complement to the nowadays available options, the PD models presented in this thesis may help to contribute to the understanding of the pathophysiology and to delineate potential neuroprotective strategies for PD.

Acknowledgments

-Acknowledgments-

I wish to express my sincere thanks to Dr. Hiroyuki Nakayama and Dr. Kazuyuki Uchida (Department of Veterinary Pathology, Graduate School of Agricultural and Life Sciences, The University of Tokyo), for giving me the opportunity to study in this magnificent university and for providing me with all the necessary facilities.

In addition, I would like to give my high, respectful gratitude to Chiyo Doi and all the professors and administrative personal of this university who have lent their helping hands in this wonderful process.

I also want to thank all the members of my family, without whom this thesis would not have been possible.

Sebastián Rodríguez

Tokyo, December 14th, 2012

References

[1] Shulman JM, De Jager PL, Feany MB. Parkinson's disease: genetics and pathogenesis. Annu Rev Pathol. 2011;6:193-222.

[2] Cai H, Cong WN, Ji S, Rothman S, Maudsley S, Martin B. Metabolic dysfunction in Alzheimer's disease and related neurodegenerative disorders. Curr Alzheimer Res. 2012;9:5-17.

[3] Hornykiewicz O. [The tropical localization and content of noradrenalin and dopamine (3-hydroxytyramine) in the substantia nigra of normal persons and patients with Parkinson's disease]. Wien Klin Wochenschr. 1963;75:309-12.

[4] Phani S, Loike JD, Przedborski S. Neurodegeneration and inflammation in Parkinson's disease. Parkinsonism Relat Disord. 2012;18 Suppl 1:S207-9.

[5] Ouchi Y, Yagi S, Yokokura M, Sakamoto M. Neuroinflammation in the living brain of Parkinson's disease. Parkinsonism Relat Disord. 2009;15 Suppl 3:S200-4.

[6] Lang AE, Lozano AM. Parkinson's disease. First of two parts. N Engl J Med. 1998;339:1044-53.

[7] Lang AE, Lozano AM. Parkinson's disease. Second of two parts. N Engl J Med. 1998;339:1130-43.

[8] Langston JW, Forno LS, Rebert CS, Irwin I. Selective nigral toxicity after systemic administration of 1-methyl-4-phenyl-1,2,5,6-tetrahydropyrine (MPTP) in the squirrel monkey. Brain Res. 1984;292:390-4.

[9] Brooks WJ, Jarvis MF, Wagner GC. Attenuation of MPTP-induced dopaminergic neurotoxicity by a serotonin uptake blocker. J Neural Transm. 1988;71:85-90.

[10] Brooks WJ, Jarvis MF, Wagner GC. Astrocytes as a primary locus for the conversion MPTP into MPP+. J Neural Transm. 1989;76:1-12.

[11] Blesa J, Phani S, Jackson-Lewis V, Przedborski S. Classic and new animal models of Parkinson's disease. J Biomed Biotechnol. 2012;2012:845618.

[12] Riachi NJ, Harik SI, Kalaria RN, Sayre LM. On the mechanisms underlying 1-methyl-4-phenyl-1,2,3,6-tetrahydropyridine neurotoxicity. II. Susceptibility among mammalian species correlates with the toxin's metabolic patterns in brain microvessels and liver. J Pharmacol Exp Ther. 1988;244:443-8.

[13] Kalaria RN, Mitchell MJ, Harik SI. Correlation of 1-methyl-4-phenyl-1,2,3,6-tetrahydropyridine neurotoxicity with blood-brain barrier monoamine oxidase activity. Proc Natl Acad Sci U S A. 1987;84:3521-5.

[14] Johannessen JN, Chiueh CC, Burns RS, Markey SP. Differences in the metabolism of MPTP in the rodent and primate parallel differences in sensitivity to its neurotoxic effects. Life Sci. 1985;36:219-24.

[15] Sundstrom E, Samuelsson EB. Comparison of key steps in 1-methyl-4-phenyl-1,2,3,6-tetrahydropyridine (MPTP) neurotoxicity in rodents. Pharmacol Toxicol. 1997;81:226-31.

[16] Mitra N, Mohanakumar KP, Ganguly DK. Resistance of golden hamster to 1-methyl-4-phenyl-1,2,3,6-tetrahydropyridine: relationship with low levels of regional monoamine oxidase B. J Neurochem. 1994;62:1906-12.

[17] Ungerstedt U. 6-Hydroxy-dopamine induced degeneration of central monoamine neurons. Eur J Pharmacol. 1968;5:107-10.

[18] Perese DA, Ulman J, Viola J, Ewing SE, Bankiewicz KS. A 6-hydroxydopamine-induced selective parkinsonian rat model. Brain Res. 1989;494:285-93.

[19] Ichitani Y, Okamura H, Matsumoto Y, Nagatsu I, Ibata Y. Degeneration of the nigral dopamine neurons after 6-hydroxydopamine injection into the rat striatum. Brain Res. 1991;549:350-3.

[20] Sauer H, Oertel WH. Progressive degeneration of nigrostriatal dopamine neurons

following intrastriatal terminal lesions with 6-hydroxydopamine: a combined retrograde tracing and immunocytochemical study in the rat. Neuroscience. 1994;59:401-15.

[21] Lee CS, Sauer H, Bjorklund A. Dopaminergic neuronal degeneration and motor impairments following axon terminal lesion by instrastriatal 6-hydroxydopamine in the rat. Neuroscience. 1996;72:641-53.

[22] Kirik D, Rosenblad C, Bjorklund A. Characterization of behavioral and neurodegenerative changes following partial lesions of the nigrostriatal dopamine system induced by intrastriatal 6-hydroxydopamine in the rat. Exp Neurol. 1998;152:259-77.

[23] Von Voigtlander PF, Moore KE. Turning behavior of mice with unilateral 6-hydroxydopamine lesions in the striatum: effects of apomorphine, L-DOPA, amanthadine, amphetamine and other psychomotor stimulants. Neuropharmacology. 1973;12:451-62.

[24] Iancu R, Mohapel P, Brundin P, Paul G. Behavioral characterization of a unilateral 6-OHDA-lesion model of Parkinson's disease in mice. Behav Brain Res. 2005;162:1-10.

[25] Cohen G, Heikkila RE. The generation of hydrogen peroxide, superoxide radical, and hydroxyl radical by 6-hydroxydopamine, dialuric acid, and related cytotoxic agents. J Biol Chem. 1974;249:2447-52.

[26] Heikkila R, Cohen G. Further studies on the generation of hydrogen peroxide by 6-hydroxydopamine. Potentiation by ascorbic acid. Mol Pharmacol. 1972;8:241-8.

[27] Jonsson G. Chemical neurotoxins as denervation tools in neurobiology. Annu Rev Neurosci. 1980;3:169-87.

[28] Sachs C, Jonsson G. Mechanisms of action of 6-hydroxydopamine. Biochem Pharmacol. 1975;24:1-8.

[29] Smith MP, Cass WA. Oxidative stress and dopamine depletion in an intrastriatal

6-hydroxydopamine model of Parkinson's disease. Neuroscience. 2007;144:1057-66.

[30] Sanchez-Iglesias S, Rey P, Mendez-Alvarez E, Labandeira-Garcia JL, Soto-Otero R. Time-course of brain oxidative damage caused by intrastriatal administration of 6-hydroxydopamine in a rat model of Parkinson's disease. Neurochem Res. 2007;32:99-105.

[31] Thoenen H, Tranzer JP. Chemical sympathectomy by selective destruction of adrenergic nerve endings with 6-Hydroxydopamine. Naunyn Schmiedebergs Arch Exp Pathol Pharmakol. 1968;261:271-88.

[32] Javoy F, Sotelo C, Herbet A, Agid Y. Specificity of dopaminergic neuronal degeneration induced by intracerebral injection of 6-hydroxydopamine in the nigrostriatal dopamine system. Brain Res. 1976;102:201-15.

[33] Jeon BS, Jackson-Lewis V, Burke RE. 6-Hydroxydopamine lesion of the rat substantia nigra: time course and morphology of cell death. Neurodegeneration. 1995;4:131-7.

[34] Garver DL, Cedarbaum J, Maas JW. Blood-brain barrier to 6-hydroxydopamine: uptake by heart and brain. Life Sci. 1975;17:1081-4.

[35] Hamre K, Tharp R, Poon K, Xiong X, Smeyne RJ. Differential strain susceptibility following 1-methyl-4-phenyl-1,2,3,6-tetrahydropyridine (MPTP) administration acts in an autosomal dominant fashion: quantitative analysis in seven strains of Mus musculus. Brain Res. 1999;828:91-103.

[36] Morin LP, Wood RI. A stereotaxic atlas of the golden hamster brain. San Diego, Calif. ; London: Academic Press; 2001.

[37] Kinemuchi H, Arai Y, Toyoshima Y. Participation of brain monoamine oxidase B form in the neurotoxicity of 1-methyl-4-phenyl-1,2,3,6-tetrahydropyridine: relationship between the enzyme inhibition and the neurotoxicity. Neurosci Lett. 1985;58:195-200.

[38] Zimmer J, Geneser FA. Difference in monoamine oxidase B activity between C57 black and albino NMRI mouse strains may explain differential effects of the neurotoxin MPTP. Neurosci Lett. 1987;78:253-8.

[39] Trevor AJ, Castagnoli N, Jr., Caldera P, Ramsay RR, Singer TP. Bioactivation of MPTP: reactive metabolites and possible biochemical sequelae. Life Sci. 1987;40:713-9.

[40] Trevor AJ, Singer TP, Ramsay RR, Castagnoli N, Jr. Processing of MPTP by monoamine oxidases: implications for molecular toxicology. J Neural Transm Suppl. 1987;23:73-89.

[41] Wu WR, Zhu XZ, Guan HJ, Wang RG, Ji XQ. Neuroprotective rather than neurorescue or neurorestorative effect of selegiline against MPTP-induced dopaminergic toxicity. Zhongguo Yao Li Xue Bao. 1999;20:146-50.

[42] Kupsch A, Sautter J, Gotz ME, Breithaupt W, Schwarz J, Youdim MB, et al. Monoamine oxidase-inhibition and MPTP-induced neurotoxicity in the non-human primate: comparison of rasagiline (TVP 1012) with selegiline. J Neural Transm. 2001;108:985-1009.

[43] Birkmayer W, Knoll J, Riederer P, Youdim MB, Hars V, Marton J. Increased life expectancy resulting from addition of L-deprenyl to Madopar treatment in Parkinson's disease: a longterm study. J Neural Transm. 1985;64:113-27.

[44] Shults CW. Effect of selegiline (deprenyl) on the progression of disability in early Parkinson's disease. Parkinson Study Group. Acta Neurol Scand Suppl. 1993;146:36-42.

[45] Smeyne RJ, Jackson-Lewis V. The MPTP model of Parkinson's disease. Brain Res Mol Brain Res. 2005;134:57-66.

[46] Kalaria RN, Harik SI. Differential postnatal development of monoamine oxidases A and B in the blood-brain barrier of the rat. J Neurochem. 1987;49:1589-94.

[47] Riachi NJ, Dietrich WD, Harik SI. Effects of internal carotid administration of MPTP on rat brain and blood-brain barrier. Brain Res. 1990;533:6-14.

[48] Hazell AS, Itzhak Y, Liu H, Norenberg MD. 1-Methyl-4-phenyl-1,2,3,6-tetrahydropyridine (MPTP) decreases glutamate uptake in cultured astrocytes. J Neurochem. 1997;68:2216-9.

[49] Kopin IJ. Features of the dopaminergic neurotoxin MPTP. Ann N Y Acad Sci. 1992;648:96-104.

[50] Marini AM, Lipsky RH, Schwartz JP, Kopin IJ. Accumulation of 1-methyl-4-phenyl-1,2,3,6-tetrahydropyridine in cultured cerebellar astrocytes. J Neurochem. 1992;58:1250-8.

[51] Sonsalla PK, Zeevalk GD, German DC. Chronic intraventricular administration of 1-methyl-4-phenylpyridinium as a progressive model of Parkinson's disease. Parkinsonism Relat Disord. 2008;14 Suppl 2:S116-8.

[52] Forno LS, DeLanney LE, Irwin I, Di Monte D, Langston JW. Astrocytes and Parkinson's disease. Prog Brain Res. 1992;94:429-36.

[53] Barcia C, Emborg ME, Hirsch EC, Herrero MT. Blood vessels and parkinsonism. Front Biosci. 2004;9:277-82.

[54] Gainetdinov RR, Fumagalli F, Jones SR, Caron MG. Dopamine transporter is required for in vivo MPTP neurotoxicity: evidence from mice lacking the transporter. J Neurochem. 1997;69:1322-5.

[55] Liu Y, Peter D, Roghani A, Schuldiner S, Prive GG, Eisenberg D, et al. A cDNA that suppresses MPP+ toxicity encodes a vesicular amine transporter. Cell. 1992;70:539-51.

[56] Gainetdinov RR, Fumagalli F, Wang YM, Jones SR, Levey AI, Miller GW, et al. Increased MPTP neurotoxicity in vesicular monoamine transporter 2 heterozygote

knockout mice. J Neurochem. 1998;70:1973-8.

[57] Takahashi N, Miner LL, Sora I, Ujike H, Revay RS, Kostic V, et al. VMAT2 knockout mice: heterozygotes display reduced amphetamine-conditioned reward, enhanced amphetamine locomotion, and enhanced MPTP toxicity. Proc Natl Acad Sci U S A. 1997;94:9938-43.

[58] Chen PC, Vargas MR, Pani AK, Smeyne RJ, Johnson DA, Kan YW, et al. Nrf2-mediated neuroprotection in the MPTP mouse model of Parkinson's disease: Critical role for the astrocyte. Proc Natl Acad Sci U S A. 2009;106:2933-8.

[59] He XJ, Nakayama H, Dong M, Yamauchi H, Ueno M, Uetsuka K, et al. Evidence of apoptosis in the subventricular zone and rostral migratory stream in the MPTP mouse model of Parkinson disease. J Neuropathol Exp Neurol. 2006;65:873-82.

[60] He XJ, Yamauchi H, Uetsuka K, Nakayama H. Neurotoxicity of MPTP to migrating neuroblasts: studies in acute and subacute mouse models of Parkinson's disease. Neurotoxicology. 2008;29:413-20.

[61] Shibui Y, He XJ, Uchida K, Nakayama H. MPTP-induced neuroblast apoptosis in the subventricular zone is not regulated by dopamine or other monoamine transporters. Neurotoxicology. 2009;30:1036-44.

[62] Przedborski S, Levivier M, Jiang H, Ferreira M, Jackson-Lewis V, Donaldson D, et al. Dose-dependent lesions of the dopaminergic nigrostriatal pathway induced by intrastriatal injection of 6-hydroxydopamine. Neuroscience. 1995;67:631-47.

[63] Berger K, Przedborski S, Cadet JL. Retrograde degeneration of nigrostriatal neurons induced by intrastriatal 6-hydroxydopamine injection in rats. Brain Res Bull. 1991;26:301-7.

[64] Cadet JL, Last R, Kostic V, Przedborski S, Jackson-Lewis V. Long-term behavioral and biochemical effects of 6-hydroxydopamine injections in rat caudate-putamen. Brain

Res Bull. 1991;26:707-13.

[65] Blandini F, Levandis G, Bazzini E, Nappi G, Armentero MT. Time-course of nigrostriatal damage, basal ganglia metabolic changes and behavioural alterations following intrastriatal injection of 6-hydroxydopamine in the rat: new clues from an old model. Eur J Neurosci. 2007;25:397-405.

[66] Sotelo C, Javoy F, Agid Y, Glowinski J. Injection of 6-hydroxydopamine in the substantia nigra of the rat. I. Morphological study. Brain Res. 1973;58:269-90.

[67] Krammer EB. Anterograde and transsynaptic degeneration 'en cascade' in basal ganglia induced by intrastriatal injection of kainic acid: an animal analogue of Huntington's disease. Brain Res. 1980;196:209-21.

[68] Lundberg C, Wictorin K, Bjorklund A. Retrograde degenerative changes in the substantia nigra pars compacta following an excitotoxic lesion of the striatum. Brain Res. 1994;644:205-12.

[69] Blum D, Torch S, Lambeng N, Nissou M, Benabid AL, Sadoul R, et al. Molecular pathways involved in the neurotoxicity of 6-OHDA, dopamine and MPTP: contribution to the apoptotic theory in Parkinson's disease. Prog Neurobiol. 2001;65:135-72.

[70] Ciliax BJ, Heilman C, Demchyshyn LL, Pristupa ZB, Ince E, Hersch SM, et al. The dopamine transporter: immunochemical characterization and localization in brain. J Neurosci. 1995;15:1714-23.

[71] Freed C, Revay R, Vaughan RA, Kriek E, Grant S, Uhl GR, et al. Dopamine transporter immunoreactivity in rat brain. J Comp Neurol. 1995;359:340-9.

[72] Kuhn K, Wellen J, Link N, Maskri L, Lubbert H, Stichel CC. The mouse MPTP model: gene expression changes in dopaminergic neurons. Eur J Neurosci. 2003;17:1-12.

[73] Ricaurte GA, Irwin I, Forno LS, DeLanney LE, Langston E, Langston JW. Aging

and 1-methyl-4-phenyl-1,2,3,6-tetrahydropyridine-induced degeneration of dopaminergic neurons in the substantia nigra. Brain Res. 1987;403:43-51.

[74] Bezard E, Dovero S, Imbert C, Boraud T, Gross CE. Spontaneous long-term compensatory dopaminergic sprouting in MPTP-treated mice. Synapse. 2000;38:363-8.

[75] Song DD, Haber SN. Striatal responses to partial dopaminergic lesion: evidence for compensatory sprouting. J Neurosci. 2000;20:5102-14.

[76] Mitsumoto Y, Watanabe A, Mori A, Koga N. Spontaneous regeneration of nigrostriatal dopaminergic neurons in MPTP-treated C57BL/6 mice. Biochem Biophys Res Commun. 1998;248:660-3.

[77] Blanchard V, Anglade P, Dziewczapolski G, Savasta M, Agid Y, Raisman-Vozari R. Dopaminergic sprouting in the rat striatum after partial lesion of the substantia nigra. Brain Res. 1996;709:319-25.

[78] Onn SP, Berger TW, Stricker EM, Zigmond MJ. Effects of intraventricular 6-hydroxydopamine on the dopaminergic innervation of striatum: histochemical and neurochemical analysis. Brain Res. 1986;376:8-19.

[79] Jackson-Lewis V, Jakowec M, Burke RE, Przedborski S. Time course and morphology of dopaminergic neuronal death caused by the neurotoxin 1-methyl-4-phenyl-1,2,3,6-tetrahydropyridine. Neurodegeneration. 1995;4:257-69.

[80] Jakowec MW, Nixon K, Hogg E, McNeill T, Petzinger GM. Tyrosine hydroxylase and dopamine transporter expression following 1-methyl-4-phenyl-1,2,3,6-tetrahydropyridine-induced neurodegeneration of the mouse nigrostriatal pathway. J Neurosci Res. 2004;76:539-50.

[81] Roberts DC, Zis AP, Fibiger HC. Ascending catecholamine pathways and amphetamine-induced locomotor activity: importance of dopamine and apparent non-involvement of norepinephrine. Brain Res. 1975;93:441-54.

[82] Kosel S, Egensperger R, von Eitzen U, Mehraein P, Graeber MB. On the question of apoptosis in the parkinsonian substantia nigra. Acta Neuropathol. 1997;93:105-8.

[83] Banati RB, Daniel SE, Blunt SB. Glial pathology but absence of apoptotic nigral neurons in long-standing Parkinson's disease. Mov Disord. 1998;13:221-7.

[84] Nakajima K, Kohsaka S. Microglia: activation and their significance in the central nervous system. J Biochem. 2001;130:169-75.

[85] de Bock F, Dornand J, Rondouin G. Release of TNF alpha in the rat hippocampus following epileptic seizures and excitotoxic neuronal damage. Neuroreport. 1996;7:1125-9.

[86] Botchkina GI, Meistrell ME, 3rd, Botchkina IL, Tracey KJ. Expression of TNF and TNF receptors (p55 and p75) in the rat brain after focal cerebral ischemia. Mol Med. 1997;3:765-81.

[87] Sriram K, Matheson JM, Benkovic SA, Miller DB, Luster MI, O'Callaghan JP. Mice deficient in TNF receptors are protected against dopaminergic neurotoxicity: implications for Parkinson's disease. Faseb J. 2002;16:1474-6.

[88] Depino AM, Earl C, Kaczmarczyk E, Ferrari C, Besedovsky H, del Rey A, et al. Microglial activation with atypical proinflammatory cytokine expression in a rat model of Parkinson's disease. Eur J Neurosci. 2003;18:2731-42.

[89] Mirza B, Hadberg H, Thomsen P, Moos T. The absence of reactive astrocytosis is indicative of a unique inflammatory process in Parkinson's disease. Neuroscience. 2000;95:425-32.

[90] Kim WG, Mohney RP, Wilson B, Jeohn GH, Liu B, Hong JS. Regional difference in susceptibility to lipopolysaccharide-induced neurotoxicity in the rat brain: role of microglia. J Neurosci. 2000;20:6309-16.

[91] Cookson MR. The biochemistry of Parkinson's disease. Annu Rev Biochem.

2005;74:29-52.

[92] Albin RL, Young AB, Penney JB. The functional anatomy of disorders of the basal ganglia. Trends Neurosci. 1995;18:63-4.

[93] McGeer PL, Itagaki S, Boyes BE, McGeer EG. Reactive microglia are positive for HLA-DR in the substantia nigra of Parkinson's and Alzheimer's disease brains. Neurology. 1988;38:1285-91.

[94] Langston JW, Forno LS, Tetrud J, Reeves AG, Kaplan JA, Karluk D. Evidence of active nerve cell degeneration in the substantia nigra of humans years after 1-methyl-4-phenyl-1,2,3,6-tetrahydropyridine exposure. Ann Neurol. 1999;46:598-605.

[95] Akiyama H, McGeer PL. Microglial response to 6-hydroxydopamine-induced substantia nigra lesions. Brain Res. 1989;489:247-53.

[96] He Y, Lee T, Leong SK. Time course of dopaminergic cell death and changes in iron, ferritin and transferrin levels in the rat substantia nigra after 6-hydroxydopamine (6-OHDA) lesioning. Free Radic Res. 1999;31:103-12.

[97] Kurkowska-Jastrzebska I, Wronska A, Kohutnicka M, Czlonkowski A, Czlonkowska A. The inflammatory reaction following 1-methyl-4-phenyl-1,2,3, 6-tetrahydropyridine intoxication in mouse. Exp Neurol. 1999;156:50-61.

[98] Kohutnicka M, Lewandowska E, Kurkowska-Jastrzebska I, Czlonkowski A, Czlonkowska A. Microglial and astrocytic involvement in a murine model of Parkinson's disease induced by 1-methyl-4-phenyl-1,2,3,6-tetrahydropyridine (MPTP). Immunopharmacology. 1998;39:167-80.

[99] Buttini M, Limonta S, Boddeke HW. Peripheral administration of lipopolysaccharide induces activation of microglial cells in rat brain. Neurochem Int. 1996;29:25-35.

[100] Hall ED. The neuroprotective pharmacology of methylprednisolone. J Neurosurg.

1992;76:13-22.

[101] Gelati M, Corsini E, Dufour A, Massa G, Giombini S, Solero CL, et al. High-dose methylprednisolone reduces cytokine-induced adhesion molecules on human brain endothelium. Can J Neurol Sci. 2000;27:241-4.

[102] Gelati M, Corsini E, De Rossi M, Masini L, Bernardi G, Massa G, et al. Methylprednisolone acts on peripheral blood mononuclear cells and endothelium in inhibiting migration phenomena in patients with multiple sclerosis. Arch Neurol. 2002;59:774-80.

[103] Yrjanheikki J, Keinanen R, Pellikka M, Hokfelt T, Koistinaho J. Tetracyclines inhibit microglial activation and are neuroprotective in global brain ischemia. Proc Natl Acad Sci U S A. 1998;95:15769-74.

[104] Tikka TM, Koistinaho JE. Minocycline provides neuroprotection against N-methyl-D-aspartate neurotoxicity by inhibiting microglia. J Immunol. 2001;166:7527-33.

[105] Sanchez Mejia RO, Ona VO, Li M, Friedlander RM. Minocycline reduces traumatic brain injury-mediated caspase-1 activation, tissue damage, and neurological dysfunction. Neurosurgery. 2001;48:1393-9; discussion 9-401.

[106] Wu DC, Jackson-Lewis V, Vila M, Tieu K, Teismann P, Vadseth C, et al. Blockade of microglial activation is neuroprotective in the 1-methyl-4-phenyl-1,2,3,6-tetrahydropyridine mouse model of Parkinson disease. J Neurosci. 2002;22:1763-71.

[107] He Y, Appel S, Le W. Minocycline inhibits microglial activation and protects nigral cells after 6-hydroxydopamine injection into mouse striatum. Brain Res. 2001;909:187-93.

[108] Yang L, Sugama S, Chirichigno JW, Gregorio J, Lorenzl S, Shin DH, et al.

Minocycline enhances MPTP toxicity to dopaminergic neurons. J Neurosci Res. 2003;74:278-85.

[109] Diguet E, Fernagut PO, Wei X, Du Y, Rouland R, Gross C, et al. Deleterious effects of minocycline in animal models of Parkinson's disease and Huntington's disease. Eur J Neurosci. 2004;19:3266-76.

[110] Qin L, Wu X, Block ML, Liu Y, Breese GR, Hong JS, et al. Systemic LPS causes chronic neuroinflammation and progressive neurodegeneration. Glia. 2007;55:453-62.

[111] Sriram K, Miller DB, O'Callaghan JP. Minocycline attenuates microglial activation but fails to mitigate striatal dopaminergic neurotoxicity: role of tumor necrosis factor-alpha. J Neurochem. 2006;96:706-18.

[112] Drechsel DA, Estevez AG, Barbeito L, Beckman JS. Nitric Oxide-Mediated Oxidative Damage and the Progressive Demise of Motor Neurons in ALS. Neurotox Res. 2012;22:251-64.

[113] Zhou C, Huang Y, Przedborski S. Oxidative stress in Parkinson's disease: a mechanism of pathogenic and therapeutic significance. Ann N Y Acad Sci. 2008;1147:93-104.

[114] Moncada S, Higgs A. The L-arginine-nitric oxide pathway. N Engl J Med. 1993;329:2002-12.

[115] Broom L, Marinova-Mutafchieva L, Sadeghian M, Davis JB, Medhurst AD, Dexter DT. Neuroprotection by the selective iNOS inhibitor GW274150 in a model of Parkinson disease. Free Radic Biol Med. 2011;50:633-40.

[116] Saha RN, Liu X, Pahan K. Up-regulation of BDNF in astrocytes by TNF-alpha: a case for the neuroprotective role of cytokine. J Neuroimmune Pharmacol. 2006;1:212-22.

[117] Kuno R, Yoshida Y, Nitta A, Nabeshima T, Wang J, Sonobe Y, et al. The role of

TNF-alpha and its receptors in the production of NGF and GDNF by astrocytes. Brain Res. 2006;1116:12-8.

[118] Chang YP, Fang KM, Lee TI, Tzeng SF. Regulation of microglial activities by glial cell line derived neurotrophic factor. J Cell Biochem. 2006;97:501-11.

[119] Nagatsu T, Sawada M. Inflammatory process in Parkinson's disease: role for cytokines. Curr Pharm Des. 2005;11:999-1016.

[120] Kirik D, Georgievska B, Bjorklund A. Localized striatal delivery of GDNF as a treatment for Parkinson disease. Nat Neurosci. 2004;7:105-10.

[121] Smith MP, Cass WA. GDNF reduces oxidative stress in a 6-hydroxydopamine model of Parkinson's disease. Neurosci Lett. 2007;412:259-63.

[122] Spina MB, Squinto SP, Miller J, Lindsay RM, Hyman C. Brain-derived neurotrophic factor protects dopamine neurons against 6-hydroxydopamine and N-methyl-4-phenylpyridinium ion toxicity: involvement of the glutathione system. J Neurochem. 1992;59:99-106.

[123] Riley CP, Cope TC, Buck CR. CNS neurotrophins are biologically active and expressed by multiple cell types. J Mol Histol. 2004;35:771-83.

[124] Barcia C, Ros CM, Annese V, Gomez A, Ros-Bernal F, Aguado-Llera D, et al. IFN-gamma signaling, with the synergistic contribution of TNF-alpha, mediates cell specific microglial and astroglial activation in experimental models of Parkinson's disease. Cell Death Dis. 2012;3:e379.

[125] Paintlia AS, Paintlia MK, Singh I, Skoff RB, Singh AK. Combination therapy of lovastatin and rolipram provides neuroprotection and promotes neurorepair in inflammatory demyelination model of multiple sclerosis. Glia. 2009;57:182-93.

[126] Chen X, Hu X, Zou Y, Pi R, Liu M, Wang T, et al. Combined treatment with minocycline and prednisone attenuates experimental autoimmune encephalomyelitis in

C57 BL/6 mice. J Neuroimmunol. 2009;210:22-9.

[127] Chen X, Pi R, Liu M, Ma X, Jiang Y, Liu Y, et al. Combination of methylprednisolone and minocycline synergistically improves experimental autoimmune encephalomyelitis in C57 BL/6 mice. J Neuroimmunol. 2010;226:104-9.